

# Plutonium Dioxide Dissolution in Glass

John D. Vienna, David L. Alexander, Hong Li, and Michael J. Schweiger  
Pacific Northwest National Laboratory, Richland, WA 99352

David K. Peeler and Thomas F. Meaker  
Savannah River Technology Center, WSRC, Aiken, SC 29801

September 1996

DISTRIBUTION OF THIS DOCUMENT IS UNLIMITED

MASTER

DISTRIBUTION OF THIS DOCUMENT IS UNLIMITED

Prepared for the U.S. Department of Energy,  
under Contract DE-AC06-76RLO 1830

Pacific Northwest National Laboratory  
Richland, Washington 99352

## Disclaimer

This report was prepared as an account of work sponsored by an agency of the United States Government. Neither the United States Government nor any agency thereof, nor Battelle Memorial Institute, nor any of their employees, makes any warranty, express or implied, or assumes any legal liability or responsibility for the accuracy, completeness, or usefulness of any information, apparatus, product, or process disclosed, or represents that its use would not infringe privately owned rights. Reference herein to any specific commercial product, process, or service by trade name, trademark, manufacturer, or otherwise does not necessarily constitute or imply its endorsement, recommendation, or favoring by the United States Government or any agency thereof, or Battelle Memorial Institute. The views and opinions of authors expressed herein do not necessarily state or reflect those of the United States Government or any agency thereof.

PACIFIC NORTHWEST NATIONAL LABORATORY  
*operated by*  
BATTELLE MEMORIAL INSTITUTE  
*for the*  
UNITED STATES DEPARTMENT OF ENERGY  
*under Contract DE-AC06-76RLO 1830*

Printed in the United States of America

Available to DOE and DOE contractors from the  
Office of Scientific and Technical Information, P.O.  
Box 62, Oak Ridge, TN 37831; prices available from  
(615) 576-8401.

Available to the public from the National Technical  
Information Service, U.S. Department of Commerce,  
5285 Port Royal Rd., Springfield, VA 22161



This document was printed on recycled paper.

**DISCLAIMER**

**Portions of this document may be illegible  
in electronic image products. Images are  
produced from the best available original  
document.**

## Executive Summary

To prove the technical and economic feasibility of the dispositioning of excess weapons usable materials by vitrification, it is necessary to demonstrate that  $\text{PuO}_2$  feedstock can be dissolved in glass in sufficient quantity and in less than 8 h. The objective of this study is to demonstrate a high  $\text{PuO}_2$  solubility in glass and to identify the rough time scale required for  $\text{PuO}_2$  dissolution in a candidate immobilization glass. The results of this study confirm that the Pu solubility can be as high as 10 wt% in glass (11.4 wt%  $\text{PuO}_2$ ) and the time required for dissolution of  $\text{PuO}_2$  in glass was less than 4 h in every case and as low as 1 to 2 h. This time requirement is based on a single glass composition and two  $\text{PuO}_2$  source materials with similar particle size distributions (PSD); one high-fired and one low-fired. Temperature, glass composition, and PSD of  $\text{PuO}_2$  are suspected being the major factors in  $\text{PuO}_2$  dissolution rates in glass. Additional tests are required to examine the effects of temperature, PSD, and glass composition on  $\text{PuO}_2$  dissolution kinetics.

## Contents

Executive Summary .....	iii
Introduction .....	1
Experimental Approach .....	1
Low-Fired PuO <sub>2</sub> Source .....	1
High-Fired PuO <sub>2</sub> Source .....	1
Frit Fabrication .....	1
Spiking and Glass Fabrication .....	2
Glass analysis .....	3
Results and Observations .....	4
Frit and Feed .....	4
Melt 1 .....	8
Melt 2 .....	9
Melt 3 .....	10
Melt 4 .....	11
Melt 5 .....	11
Melt 6 .....	12
Glass Composition .....	12
Summary and Discussion .....	14
Acknowledgements .....	15
References .....	15
Distribution .....	16
Appendix A — X-Ray Diffraction Results .....	A-1
Appendix B — Inductively Coupled Plasma / Mass Spectroscopy Results .....	A-38
Appendix C — Radiochemical Analysis Results .....	A-40

### List of Figures

Figure 1. Photomicrograph (SEM) of low-fired oxide crucible feed material .....	7
Figure 2. Photomicrograph (SEM) of high-fired oxide crucible feed material .....	7
Figure 3. Unsuccessful attempt to stir hot glass .....	8
Figure 4. Melt 1 glass photograph .....	9
Figure 5. Successful stir of hot glass .....	9
Figure 6. Melt 2 glass photograph .....	10
Figure 7. Melt 3 glass photograph .....	10
Figure 8. Melt 4 glass photograph .....	11
Figure 9. Melt 5 glass photograph .....	11

### List of Tables

Table I. Frit and glass composition (as batched) .....	2
Table II. Melting history for six LaBS glasses .....	3
Table III. Glass sample identification. ....	4
Table IV. Viscosity temperature data for LaBS frit .....	5
Table V. Isotopics of Pu feed materials by radiochemical analysis .....	6
Table VI. Particle size distributions of PuO <sub>2</sub> in crucible feed materials .....	8
Table VII. Mass spectroscopic analysis of glass composition .....	12
Table VIII. Alpha energy analysis of glass samples .....	13
Table IX. Mass percent isotopics of glass samples .....	13
Table X. Mass percent Pu and PuO <sub>2</sub> in glass samples .....	13

## Introduction

In the aftermath of the Cold War, the U.S. Department of Energy's (DOE) Office of Fissile Materials Disposition (OFMD) is charged with providing technical support for evaluation of disposition options for excess fissile materials manufactured for the nation's defense. One option being considered for the disposition of excess plutonium (Pu) is immobilization by vitrification. The vitrification option entails immobilizing Pu in a host glass and waste package that are criticality-safe (immune to nuclear criticality), proliferation-resistant, and environmentally acceptable for long-term storage or disposal.

To prove the technical and economic feasibility of candidate vitrification options it is necessary to demonstrate that PuO<sub>2</sub> feedstock can be dissolved in glass in sufficient quantity. The OFMD immobilization program has set a Pu solubility goal of 10 wt% in glass. The life cycle cost of the vitrification options are strongly influenced by the rate at which PuO<sub>2</sub> dissolves in glass (DOE 1996). The total number of process lines needed for vitrification of 50 t of Pu in 10 years is directly dependent upon the time required for Pu dissolution in glass.

The objective of this joint Pacific Northwest National Laboratory (PNNL) - Savannah River Technology Center (SRTC) study was to demonstrate a high Pu solubility in glass and to identify on a rough scale the time required for Pu dissolution in the glass. This study was conducted using a lanthanide borosilicate (LaBS) glass composition designed at the SRTC for the vitrification of actinides (Bibler et al. 1996).

## Experimental Approach

### *Low-Fired PuO<sub>2</sub> Source*

The source Pu for low-fired oxide testing was obtained from a 20.2 g/L 0.35 *M* nitric acid solution (Pu blend 1). The solution was boiled in roughly 0.25 L batches in a teflon container at a temperature increasing from 200 to 270°C as the volume was reduced. Once a ten-fold reduction in volume was achieved, the liquid was transferred to an alumina crucible and heated in a muffle furnace between 270 and 300°C, forming a thick foamy paste which was then completely dried. The dried Pu nitrate powder was calcined between 350 and 400°C for over 30 minutes for direct conversion to PuO<sub>2</sub> according to the procedure in Wick (1980). Visual inspection of the calcined PuO<sub>2</sub> showed a fine powder which was brownish green in color. Radiochemical analysis was performed to obtain material isotopics and mass fraction Pu (see Glass Composition Section).

### *High-Fired PuO<sub>2</sub> Source*

The source Pu for high-fired oxide testing was taken from a material lot of material with unknown history labeled "high-fired PuO<sub>2</sub>." An 89 g sample of the material was placed in a MgO crucible, fired at 1000°C for over 2 h, and rapidly cooled to room temperature. Radiochemical analysis was performed (see Glass Composition Section) to obtain material isotopics and mass fraction Pu in the oxide material.

### *Frit Fabrication*

The frit composition listed in Table I and used in this study is based on current work at

SRTC regarding optimization of Pu solubility within the LaBS system. This frit (without PuO<sub>2</sub>) was fabricated according to standard test procedures (Hirma et al. 1994). A 500 g batch of frit was melted at 1450°C for 1 h in a covered Pt/Rh crucible, steel quenched, and ground in a tungsten carbide mill for 3 min. The viscosity-temperature curve for this frit was measured using a spindle type viscometer according to standard test procedures (Hirma et al. 1994) and augmented with two data points from a beam bending viscometer at low temperature.

**Table I.** LaBS frit and glass composition (as batched)

Oxide	wt% in Frit	wt% in Glass	Source Chemical
SiO <sub>2</sub>	29.13	25.80	SiO <sub>2</sub>
B <sub>2</sub> O <sub>3</sub>	11.74	10.40	H <sub>3</sub> BO <sub>3</sub>
Al <sub>2</sub> O <sub>3</sub>	21.49	19.04	Al <sub>2</sub> O <sub>3</sub>
ZrO <sub>2</sub>	1.30	1.15	ZrO <sub>2</sub>
Gd <sub>2</sub> O <sub>3</sub>	8.59	7.61	Gd <sub>2</sub> O <sub>3</sub>
La <sub>2</sub> O <sub>3</sub>	12.43	11.01	La <sub>2</sub> O <sub>3</sub>
Nd <sub>2</sub> O <sub>3</sub>	12.84	11.37	Nd <sub>2</sub> O <sub>3</sub>
<b>PuO<sub>2</sub></b>	<b>0.00</b>	<b>11.39</b>	<b>PuO<sub>2</sub></b>
SrO	2.50	2.22	SrCO <sub>3</sub>

### *Spiking and Glass Fabrication*

Six glass melts were made to assess the effect of time, temperature, and stirring on the dissolution of PuO<sub>2</sub> into the LaBS glass. The targeted glass composition is shown in Table I. The targeted 11.39 wt% PuO<sub>2</sub> translates to 10.1 wt% of elemental Pu in the target glass composition. For each melt, 4.5 g of PuO<sub>2</sub> was added to 35.5 g of frit to produce 40.0 g of glass. The frit/PuO<sub>2</sub> mixture was manually stirred, milled in an automated Al<sub>2</sub>O<sub>3</sub> mortar and pestle for 1.75 min, and loaded in a covered Pt/Rh crucible for melting. The melt feeds (milled mixture of PuO<sub>2</sub> and frit) were analyzed using scanning electron microscopy (SEM) to characterize particle size distribution (PSD) of frit and PuO<sub>2</sub>, mixedness, and morphology. Table II summarizes the melt history for the six melts.



**Table II.** Melting history for six LaBS glasses

Melt #	Temperature	Time	Agitation	PuO <sub>2</sub> Feed	Appearance
1	1450°C	4 h	static	low-fired	layered
2	1500	4	stirred*	low-fired	homogeneous
3	1500	2	stirred*	low-fired	homogeneous
4	1500	4	static	low-fired	homogeneous
5	1500	1	stirred*	low-fired	layered
6	1500	4	stirred*	high-fired	homogeneous

\*Melts were manually stirred twice during each melt using an Inconel rod for approximately 5 seconds.

### *Glass analysis*

For each glass that visually appeared homogeneous, a representative sample containing bottom, top, and crucible side wall surfaces were obtained. For those samples that were actually composed of distinct layers (e.g., a layer of undissolved PuO<sub>2</sub> on the bottom surface), representative samples from the top and bottom surfaces were taken and analyzed. Table III summarizes the analyses performed for each sample. For example, Melt #1 (1450°C, 4 h, static, low fired) visually had two distinct layers. A representative sample from the top (bulk) glass (sample V-4) and the undissolved layer (sample V-6) were taken for analysis. Sample V-4 was submitted for ICP/MS, XRD, and radiochemistry.

For x-ray diffraction (XRD) analysis, the samples were milled and the powder was mixed with collodion and amyl acetate and then transferred to a glass slide. The amyl acetate was dried, leaving the glass sample "glued" to the slide with collodion. A fast XRD scan was performed on each sample from 10 to 80° two-theta with a 3 s dwell and 0.05° step size. A slow scan was performed on each sample from 25 to 35° two-theta with a 20 s dwell and 0.02° step size. The slow scan was performed over the 100% peak for PuO<sub>2</sub> (JCPDS card # 41-1170) to give increased sensitivity to undissolved PuO<sub>2</sub>. Calibration of the slow scan procedure has yielded an estimated PuO<sub>2</sub> detection limit of 0.20 wt%.

**Table III.** Glass sample identification.

Sample #	Melt #	Portion of Melt	Analyses Performed
V-1	2	top to bottom	ICP/MS, XRD, Radiochemistry
V-2	4	top to bottom	ICP/MS, XRD, Radiochemistry
V-3	3	top to bottom	ICP/MS, XRD, Radiochemistry
V-4	1	top	ICP/MS, XRD, Radiochemistry
V-5	5	top	ICP/MS, XRD, Radiochemistry
V-6	1	bottom	XRD
V-7	5	bottom	XRD
V-8	6	top to bottom	XRD, Radiochemistry

Glass composition was measured from the same representative samples that were fused in KOH in a Ni crucible. The solution was diluted to 1000X and analyzed using an inductively coupled plasma - mass spectrometer (ICP/MS). The relative error for these samples was determined to be 15% for all elements except Al, which was subject to higher error. Equipment problems prohibited the measurement of Si in the sample. Radiochemistry was also performed on the starting nitrate and high-fired oxide feeds and on the fused glass samples with total alpha and gamma energy analysis and mass spectroscopy with a relative error of 6% or less for alpha analysis.

## Results and Observations

### *Frit and Feed*

The viscosity-temperature data of the frit is reported in Table IV. This data has been fitted to both Arrhenius (1) and Fulcher (2) viscosity equations:

$$\ln(\eta) = A + \frac{B}{T}, \quad (1)$$

and

$$\ln(\eta) = E + \frac{F}{T - T_0}, \quad (2)$$

where the constants A, B, E, F, and  $T_0$  are -21.67, 38152 K, -9.88, 10023 K, and 764.0 K, respectively. The Arrhenian activation energy for viscous flow is estimated at 1350°C to be 317 KJ/mol. The two melting temperatures 1450 and 1500°C correspond to viscosities of 2.05 and 1.33 Pa·s, respectively (as predicted by the Fulcher equation). With an Arrhenius activation temperature of 38152 K, the frit is considered to be extremely short compared to average high-level waste (HLW) glass with an activation temperature near 20000 K.

**Table IV.** Viscosity temperature data for LaBS frit

T (°C)	$\eta$ (Pa·s)
1386	3.89
1337	7.14
1288	13.28
1336	7.18
1386	3.92
1435	2.30
1386	3.98
1239	29.37
1190	81.49
1140	259.02
782	$6.5 \times 10^{10}$
765	$3.0 \times 10^{11}$

The radiochemical analysis of the nitrate and high-fired oxide feedstocks are given in Table V. The nitrate results show a solution concentration of 20.2 g/L of actinides with 6.4 wt%  $^{240}\text{Pu}$ . Upon calcination of the 1.0 L of feed material, 22.82 g of  $\text{PuO}_2$  were obtained which, when compared with the 22.88 g of  $\text{PuO}_2$  expected from radiochemical analysis, suggests little impurity in the  $\text{PuO}_2$  feed.

**Table V.** Isotopics of Pu feed materials by radiochemical analysis

	Nitrate Solution (g/L <sub>Soln</sub> )	High-Fired Oxide (g/g <sub>Oxide</sub> )
<sup>238</sup> Pu	0.0000	0.0006
<sup>239</sup> Pu	0.1884	0.7550
<sup>240</sup> Pu	0.0129	0.0829
<sup>241</sup> Pu	0.0004	0.0005
<sup>241</sup> Am	0.0000	0.0023
<sup>242</sup> Pu	0.0001	0.0439
Total	0.2018	0.8851

The radiochemical analysis results of the high-fired oxide feed show a concentration of 88.51 g per 100 g of oxide with 8.3 wt% <sup>240</sup>Pu. Assuming the Pu is in the Pu<sup>4+</sup> state in the oxide, oxygen will make up 11.8 g per 100 g of oxide, suggesting that the impurity level in this PuO<sub>2</sub> feed is below detectable limits by this method.

Electron micrographs of the low-fired and high-fired oxide/frit mixtures are shown in Figures 1 and 2, respectively. The particle size distributions of the low- and high-fired oxides are listed in Table VI. For both feeds the particle size ranges from submicron to 5 μm. The high-fired oxide has slightly smaller particles with a weight average size of 2.7 μm compared to 3.8 μm for the low-fired oxide. The PSD is broader for the high-fired oxide with a 14.4 % width at half max compared to 4.5 % for the low-fired oxide. In both feeds, the frit material is was in the 10 to 50 μm range and well mixed with the smaller PuO<sub>2</sub> particles.

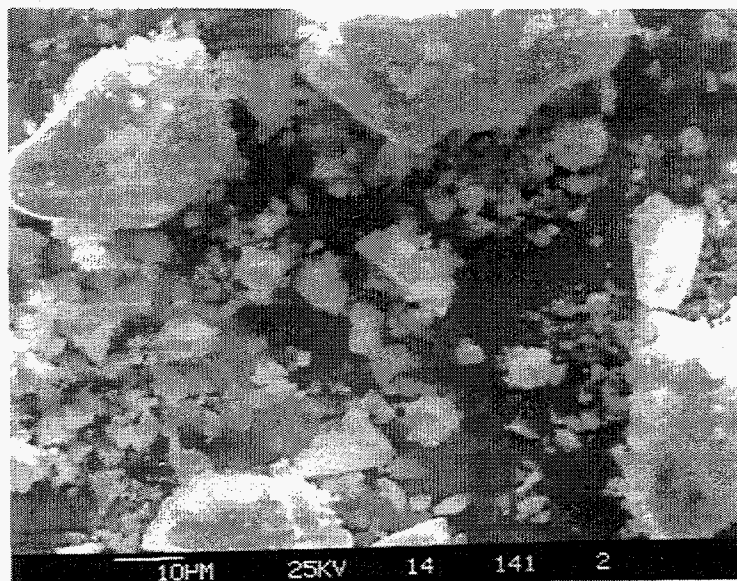


**Figure 1.** Photomicrograph (SEM) of low-fired oxide crucible feed material

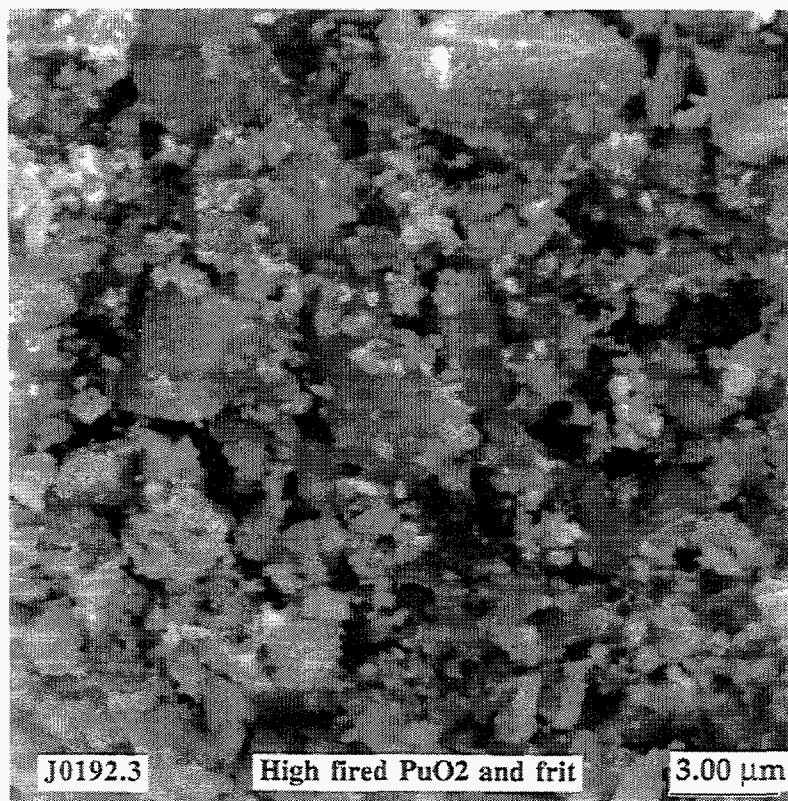


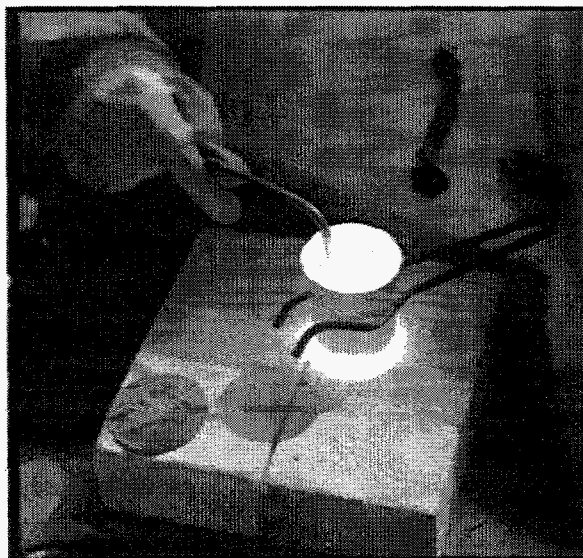
**Figure 2.** Photomicrograph (SEM) of high-fired oxide crucible feed material

**Table VI.** Particle size distributions of PuO<sub>2</sub> in crucible feed materials

Discrete Sizes	High-Fired Oxide % Count	Low-Fired Oxide % Count	High-Fired Oxide Mass %	Low-Fired Oxide Mass %
0.0-0.5 $\mu\text{m}$	91.4	25.0	4.3	0.2
0.5-1.0 $\mu\text{m}$	5.3	28.8	4.0	1.7
1.0-1.5 $\mu\text{m}$	1.1	15.9	4.0	3.5
1.5-2.0 $\mu\text{m}$	0.5	9.8	11.4	5.2
2.0-3.0 $\mu\text{m}$	0.5	8.3	15.8	11.4
3.0-5.0 $\mu\text{m}$	1.1	12.1	60.5	78.0

*Melt 1*

The first melt was performed at 1450°C for 4 h under static conditions. After 1 h of melting, the glass was removed from the furnace for stirring. However, due to the low melting temperature, the high activation energy for viscous flow, and the relatively long period before stirring was attempted, the glass was far too viscous to stir (an estimated viscosity of 25 - 100 Pa·s). It was returned to the furnace and an attempt was made to stir at 2 h. This attempt was again unsuccessful as shown in Figure 3.

**Figure 3.** Unsuccessful attempt to stir hot glass

After 4 h of melting the glass was removed from the furnace and quenched by partially submerging the crucible in a water bath. The resulting glass was clear and dark green in color with

a thin (~ 0.25 mm) layer of brownish green crystals at the bottom of the melt. Figure 4 shows representative samples of the top and bottom layer. The XRD results for all samples are shown in Appendix A. According to XRD the top layer (sample V-4) is amorphous while the bottom layer (sample V-6) contains crystalline  $\text{PuO}_2$ . Radiochemical and XRD analyses show that  $8.32 \pm 0.50$  wt% Pu (or  $9.44 \pm 0.57$  wt%  $\text{PuO}_2$ ) was dissolved in the top amorphous layer of the glass.

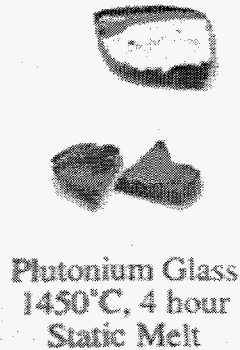


**Figure 4.** Melt 1 glass photograph

#### *Melt 2*

The second melt was performed at 1500°C for 4 h. After 1 h of melting the glass was removed from the furnace for stirring. The glass viscosity was reasonably low with an estimated viscosity of 3 - 8 Pa·s. The glass was stirred manually with an inconel stir rod for approximately 5-10 s. It was returned to the furnace and stirred again at 2 h. The successful stirring is shown in Figure 5.



**Figure 5.** Successful stir of hot glass

After 4 h of melting the glass was transparent and dark green in color with no apparent

layer at the bottom of the melt. Figure 6 shows representative samples of the glass viewed from the top (above) and the bottom (below). The XRD analysis of sample V-1 shows the sample is amorphous. Radiochemical and XRD analyses show that  $10.11 \pm 0.61$  wt% Pu (or  $11.47 \pm 0.69$  wt%  $\text{PuO}_2$ ) was completely dissolved in the glass.

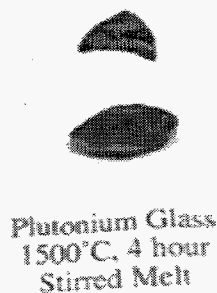


**Figure 6.** Melt 2 glass photograph

### *Melt 3*

The third melt was performed at 1500°C for 2 h. After 40 min of melting, the glass was removed from the furnace for stirring. The glass viscosity was reasonably low and the stir was successful (an estimated viscosity of 3 - 8 Pa·s). It was returned to the furnace and stirred again at 80 min.

After 2 h of melting, the glass was clear and dark green in color with no apparent layer at the bottom of the melt. Figure 7 shows representative samples of the glass with the top view on top and the bottom view on bottom. The XRD analysis of sample V-3 shows the sample is amorphous. Radiochemical and XRD analyses show that  $9.78 \pm 0.59$  wt% Pu (or  $11.09 \pm 0.67$  wt%  $\text{PuO}_2$ ) was completely dissolved in the glass. A concentration of 10 wt% Pu is assumed, based on batching records and the large experimental errors associated with composition analyses.

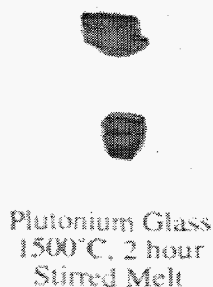


**Figure 7.** Melt 3 glass photograph



*Melt 4*

The fourth melt was performed at 1500°C for 4 h under static conditions. After 4 h of melting, the glass was clear and dark green in color with no apparent layer at the bottom of the melt. Figure 8 shows representative samples of the glass with the top view on top and the bottom view on bottom. The XRD analysis of sample V-2 shows the sample is amorphous. Radiochemical and XRD analyses show that  $10.12 \pm 0.61$  wt% Pu (or  $11.47 \pm 0.69$  wt% PuO<sub>2</sub>) was completely dissolved in the glass.

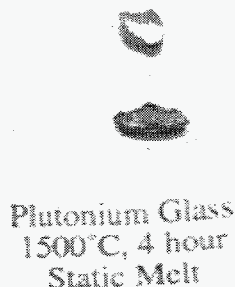


**Figure 8.** Melt 4 glass photograph

*Melt 5*

The fifth melt was performed at 1500°C for 1 h. After 20 min of melting, the glass was removed from the furnace for stirring. The glass viscosity was reasonably low and the stir was successful (an estimated viscosity of 3 - 8 Pa-s). It was returned to the furnace and stirred again at 40 min.

After 1 h of melting, the glass was clear and dark green in color with a thin (~ 0.5 mm) layer of brownish green crystals at the bottom of the melt. Figure 9 show representative samples of the glass with the top layer on top and the bottom layer on bottom. The XRD results show the top layer of glass (sample V-5) is amorphous while the bottom layer (sample V-7) contains crystalline PuO<sub>2</sub>. Radiochemical and XRD analyses show that  $9.81 \pm 0.59$  wt% Pu (or  $11.13 \pm 0.67$  wt% PuO<sub>2</sub>) was dissolved in the top amorphous layer of the glass.

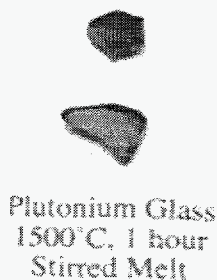


**Figure 9.** Melt 5 glass photograph

*Melt 6*

The sixth melt was performed at 1500°C for 4 h. After 1 h of melting the glass was removed from the furnace for stirring. The glass viscosity was reasonably low with an estimated viscosity of 3 - 8 Pa·s. The glass was stirred manually with an inconel stir rod for approximately 5-10 s. It was returned to the furnace and stirred again at 2 h. After 4 h of melting the glass was clear and dark green in color with no apparent layer at the bottom of the melt. The XRD analysis of sample V-8 shows the sample is amorphous. Radiochemical analyses were performed on four samples of this glass (V-8 a-d). The first two samples V-8a and b contained a portion of the melt top surface and no bottom surface. The final two samples V-8c and d contained a portion of the melt bottom surface and no top surface. By taking samples in this manner we attempted to gather Pu concentration information from different melt depths for analysis. These data show a concentration ranging from  $5.2 \pm 0.1$  wt% Pu (or  $5.9 \pm 0.1$  wt% PuO<sub>2</sub>) near the melt top to  $11.8 \pm 0.2$  wt% Pu (or  $13.4 \pm 0.3$  wt% PuO<sub>2</sub>) near the crucible bottom.

*Glass Composition*

The analyzed sample compositions are listed in Table VII. These analyses are subjected to a relative error of 15% for all components except for Al. Analysis was not completed for Si due to equipment failure. Except for Pu and Zr, all components in all samples match the batched composition within the experimental error. Low concentration readings for Pu and Zr, which are highly refractory and traditionally have been difficult to analyze by ICP/MS of KOH fused samples, can likely be dismissed. Due to the high level of experimental error of glass composition analysis, no conclusions are drawn on these results. Radiochemical analysis of Pu in glass samples given in Tables VIII and IX confirm this conclusion. Table X shows Pu and PuO<sub>2</sub> concentrations in glass based on radiochemical results.

**Table VII.** Mass spectroscopic analysis of glass composition in mass fraction

	Target	V-1	V-2	V-3	V-4	V-5
SiO <sub>2</sub>	0.258					
B <sub>2</sub> O <sub>3</sub>	0.104	0.090	0.104	0.094	0.100	0.105
Al <sub>2</sub> O <sub>3</sub>	0.190	0.223	0.221	0.202	0.225	0.217
SrO	0.022	0.021	0.023	0.019	0.022	0.022
ZrO <sub>2</sub>	0.012	0.009	0.011	0.009	0.010	0.009
La <sub>2</sub> O <sub>3</sub>	0.110	0.097	0.114	0.092	0.100	0.103
Nd <sub>2</sub> O <sub>3</sub>	0.114	0.106	0.117	0.102	0.113	0.110
Gd <sub>2</sub> O <sub>3</sub>	0.076	0.067	0.078	0.064	0.068	0.073
<sup>239</sup> PuO <sub>2</sub>	0.106	0.086	0.092	0.086	0.075	0.081
otherPuO <sub>2</sub>	0.008					
Total	1.000	0.700	0.760	0.668	0.713	0.721

**Table VIII.** Alpha energy analysis of glass samples

Sample	Alpha ( $\mu\text{Ci/g}$ )	Error (+/-)
V-1	7,470	6%
V-2	7,450	6%
V-3	7,260	6%
V-4	6,150	6%
V-5	7,210	6%
V-5 dup	7,340	6%

**Table IX.** Mass percent isotopics of glass samples

Mass	238	239	240	241	242
V-1	0.013	93.340	6.411	0.194	0.042
V-2	0.011	93.349	6.415	0.189	0.036
V-3	0.015	93.362	6.387	0.197	0.039
V-4	0.013	93.383	6.375	0.193	0.036
V-5	0.014	93.338	6.415	0.190	0.042
V-8	0.010	96.012	2.859	0.137*	1.059

\*0.076 wt%  $^{241}\text{Am}$  included in 241 for high-fired oxide**Table X.** Mass percent Pu and  $\text{PuO}_2$  in glass samples

	wt% Pu	wt% $\text{PuO}_2$	Error
V-1	10.11	11.47	6%
V-2	10.12	11.47	6%
V-3	9.78	11.09	6%
V-4	8.32	9.44	6%
V-5	9.81	11.13	6%
V-8a	5.16	5.86	2%
V-8b	7.77	8.82	2%
V-8c	11.78	13.36	2%
V-8d	10.55	11.97	2%

## Summary and Discussion

The results of this study confirm that the Pu solubility can be as high as 11.8 wt% in glass (13.4 wt% PuO<sub>2</sub>). To date this is the highest reported solubility of Pu in any glass. This glass also contains a 1:1 molar ratio of lanthanide neutron absorbers (i.e., Gd) to Pu. High solubility was consistently shown in the six test glasses which ranged from 11.8 to 5.6 wt% Pu.

The time required for dissolution of the low-fired PuO<sub>2</sub> in glass was between 1 and 2 h at 1500°C with stirring. Without stirring, the dissolution was complete in less than 4 h at 1500°C and wasn't complete in 4 h at 1450°C. The time required for dissolution of the high-fired PuO<sub>2</sub> in glass was less than 4 h at 1500°C with stirring. These time requirements are based on the glass composition tested and the particle size distributions of source of PuO<sub>2</sub> as described above.

PuO<sub>2</sub> settling rate plays a major role in determining the extent of dissolution. Once settled, dissolution of PuO<sub>2</sub> in glass will be impaired. Particle settling rate is controlled by radius ( $r$ ) to a greater extent than fluidity ( $1/\eta$ ) as seen in Stokes settling equation (assuming spherical particles settling unhindered in a convection free viscous liquid):

$$\frac{dx}{dt} = \frac{2}{9} \frac{\Delta\rho g r^2}{\eta}, \quad (3)$$

where  $x$  is distance settled,  $t$  is time,  $\Delta\rho$  is density difference, and  $g$  is acceleration due to gravity. According to Equation (3) the time required for a particle to settle,  $t_s$ , a distance,  $x$ , is proportional to  $\eta / r^2\Delta\rho$ .

The time required for a particle to dissolve in glass,  $t_D$ , is proportional to  $r\delta / D\Delta c$ , where  $\delta$  is the diffuse layer width,  $D$  is the diffusion coefficient, and  $\Delta c$  is the degree of undersaturation in the glass. Thus, for a particle to dissolve before it settles to the bottom of the crucible  $t_D \leq t_s$ , or:

$$\frac{r\delta}{KD\Delta c} \leq \frac{x\eta}{kr^2\Delta\rho g}, \quad (4)$$

where  $K$  and  $k$  are constants. The diffusion coefficient is often taken to be inversely proportional to  $\eta$  (Stokes-Einstein relationship), further simplifying the relationship between  $t_s$  and  $t_D$ . Thus to first approximation,  $t_s / t_D \propto r^3$ , and independent of  $\eta$ .

The Pu dissolved in the high-fired oxide melt was not homogeneously distributed throughout the melt. The bottom of the melt was found to be richer in Pu than the top. This phenomenon is commonly observed in the melting of "lead crystal" glass melts where lead is richer at the crucible bottom.

## Acknowledgements

The authors would like to thank the individuals whose help in this study was invaluable for its eventual success. In particular, our gratitude goes to Pavel Hrma for many helpful discussions of the data, Evan Jenson for his expert analysis of glass crystallinity, Eric Wyse for mass spectroscopy of samples, Joel Tingey and Don Rinehart for their assistance in performing the study, Rick Steele for timely sample preparation and transfer, and Jarrod Crum for particle size distribution analysis.

## References

DOE, (1996) *Technical Summary Report for Surplus Weapons-Usable Plutonium Disposition*, DOE/MD-0003, United States Department of Energy, Office of Fissile Materials Disposition, Washington DC.

P. R. Hrma, G. F. Piepel, M. J. Schweiger, D. E. Smith, D. S. Kim, P. E. Redgate, J. D. Vienna, C. A. LoPresti, D. B. Simpson, D. K. Peeler, and M. H. Langowski, (1994) *Property / Composition Relationships for Hanford High-Level Waste Glasses Melting at 1150°C*, Vol. 1, PNL-10359, Pacific Northwest National Laboratory, Richland, WA.

N. E. Bibler, W. G. Ramsey, T. F. Meaker, and J. M. Pareizs, (1996) "Durabilities of Radioactive Glasses for Immobilization of Excess Actinides at the Savannah River Site," *Mat. Res. Symp. Proc.*, Vol. 412, *Scientific Basis for Nuclear Waste Management XIX*, Materials Research Society, Pittsburgh, PA, pp. 65-72.

O. J. Wick, (1980) *Plutonium Handbook*, The American Nuclear Society, LaGrange Park, IL.

**Distribution**

<u>no. of copies</u>	<u>no. of copies</u>
2 DOE/Office Of Scientific and Technical Information	6 Lawrence Livermore National Laboratory University of California 7000 East Ave. Livermore, CA 94551
2 DOE/Office of Fissile Materials Disposition Forrestal Building 1000 Independence Ave., S.W. Washington, DC 20585	G. A. Armantrout W. L. Bourcier L. W. Gray T. Kan J. N. Kass H. F. Shaw
A. K. Caponiti W. J. Danker	
4 DOE/Richland Operations Office Richland, WA 99352	6 Westinghouse Hanford Company PO Box 1970 Richland, WA 99352
A. B. Joy J. E. Mecca R. S. Ollero C. R. Richins	T. W. Crawford R. C. Hoyt D. C. Lini R. W. Szempruch T. J. Venetz R. A. Watrous
3 Argonne National Laboratory 9700 S. Cass Ave. Argonne, IL 60439	
J. K. Bates D. B. Chamberlain D. M. Strachan	29 Pacific Northwest National Laboratory PO Box 999, Battelle Blvd. Richland, WA 99352
20 Savannah River Technology Center Westinghouse Savannah River Company Aiken, SC 29801	Document Management Files (5) D. L. Alexander J. L. Buelt M. L. Elliott D. L. Haggard P. R. Hrma E. D. Jenson H. Li J. M. Perez M. E. Peterson M. J. Schweiger L. J. Sealock R. T. Steele J. M. Tingey J. D. Vienna (10) W. J. Weber
N. E. Bibler D. A. Crowley E. F. Duhn E. W. Holtzscheiter J. C. Marra T. F. Meaker L. M. Papouchado J. M. Pareizs D. K. Peeler (10) M. J. Plodinec I. K. Sullivan	

## Appendix A

### X-Ray Diffraction Results

The following figures show the XRD scans from glass samples listed in Table III. The glasses were prepared and analyzed according to the procedures listed above.

Date September 16, 1996

To J. D. Vienna

Author Ed Jensen 9/17/96

From E. D. Jensen

Reviewer Renee Russell 9/17/96

Subject XRD Examination of Glasses Containing PuO<sub>2</sub>, Rev 1

### Summary

Eight samples of glass containing PuO<sub>2</sub> were examined using X-ray diffraction to determine which samples had crystalline PuO<sub>2</sub> present. Only glasses V6 and V7 contained a detectable amount of crystalline PuO<sub>2</sub>.

### Sample Identification

<u>Sample</u>	<u>Description</u>	<u>File Name</u>
V1	1500 deg, 4 hr, stirred	960711A, B
V2	1500 deg, 4 hr, static	960718A and 960806A
V3	1500 deg, 2 hr, stirred	960722A, B
V4	1450 deg, 4 hr, static, top layer	960802A, B
V5	1500 deg, 1 hr, stirred, top layer	960731A, B
V6	1450 deg, 4 hr, static, bottom layer	960730A, B
V7	1500 deg, 1 hr, stirred, bottom layer	960801A, B
V8	1550 deg, 4 hr, stirred, high fired	960911A, B

### Data

Raw data plots over the full range covered (short count time) for the above samples are shown in Figures 1 through 7 and 30. Figures 8 through 14 and 31 show the raw data plots for the 25 to 35 degree range (long count time). Background subtracted data are shown in Figures 15 through 21 and 32 (short count, full range) and 22 through 28 and 33 (long count, short range). "Stick figure" displays of the PuO<sub>2</sub> pattern, ICDD card 41-1170, are shown beneath the background subtracted data. Figure 34 shows an expanded view of the 53 degree range of sample V8.

A sample containing 3% PuO<sub>2</sub>, with no heat treatment, was prepared to get an estimate of the detectability limit. This sample gave a peak height (of the 28 degree line) of 3479±116 (standard deviation is 2 sigma) above background. Based on a background of 4753±110, a concentration of 0.2% PuO<sub>2</sub> should be the minimum detectable concentration under these conditions. The calculation is as follows:

$$\% = 2 * \text{sqr}((58)^2 + (55^2)) * 3\% / 3479 = 0.2\%$$

This figure applies to a sample of the same area exposed to the x-ray beam and the same thickness, since a major portion of the beam



is expected to pass through the sample. Figure 29 shows the plot from the 3% PuO<sub>2</sub> in glass sample.

The degree of crystallinity of samples V6 and V7 could not be determined since the blank data (from microscope slide + collodion) showed higher counting rates than the sample.

Sample V8, Figure 32, shows some apparent peaks at 40.6, 53.1, 61.6 and 65.9 degrees 2-theta. These are difficult to see in the raw data. The 40.6 and 65.9 degree apparent peaks are less than the 2-sigma noise value of the adjacent data, therefore these apparent peaks can be rejected as not real. The 53.1 and 61.6 degree apparent peaks exceed the 2-sigma noise level, but not the 3-sigma level in the raw data, therefore raising the question as to their reality. Detailed examination of the raw data shows the apparent peaks are really a series of adjacent points with intensities within the 2-sigma range but each having nearly the same value near the high end of the 2-sigma range. In the smoothing process, nearby data was smoothed to a value near the average, but the apparent peak points smoothed to a little higher value giving the appearance of a peak. An expanded view of the 53.1 degree range raw data is given in Figure 33, showing the lack of a real peak in this range.

#### Experimental

Samples V1, V2, V5, V6, V7 and V8 were prepared in the Process Chemistry fume hood adjacent to the glove box in which the glasses were fabricated. Samples V3 and V4 were prepared in the ACL hot cells in the 325 building. In each case 10 to 20 mg of the sample was placed in a glass container (or boron carbide mortar), a few drops of 5% collodion in amyl acetate were added and mixed to form a smooth slurry, then the slurry was transferred to a glass slide and the solvent allowed to evaporate.

The sample was examined using the Scintag PAD V XRD in room 409 of the 325 building, property number WB81320. Running conditions for the short count, full range run were 0.05 degree 2-theta step size at 1 degree/minute speed with a range of 5 to 75 degrees, except sample V1 which had 20 to 60 and sample V2 which had 5 to 70 degrees. The long count time, short range runs had parameters of 0.02 degrees 2-theta step size, 20 seconds per step counting time with a range of 25 to 35 degrees 2-theta. X-ray parameters were 45 Kv and 40 ma with a copper anode. Slits were 4, 2, 0.5 and 0.3 mm. The XRD was within calibration at all times as shown by the daily calibration check.

The work was performed to technical procedure PNL-ALO-268, Solids Analysis, X-ray Diffraction. Calibration data are in PNL LRB 53224. Daily calibration check data are in the operators notebook.

<960711A.RD> V1, Scan: 20.0-60.0/0.05, Dwell=3(sec), Anode=CU(45 kV, 40 mA), 07-11-96@09:08

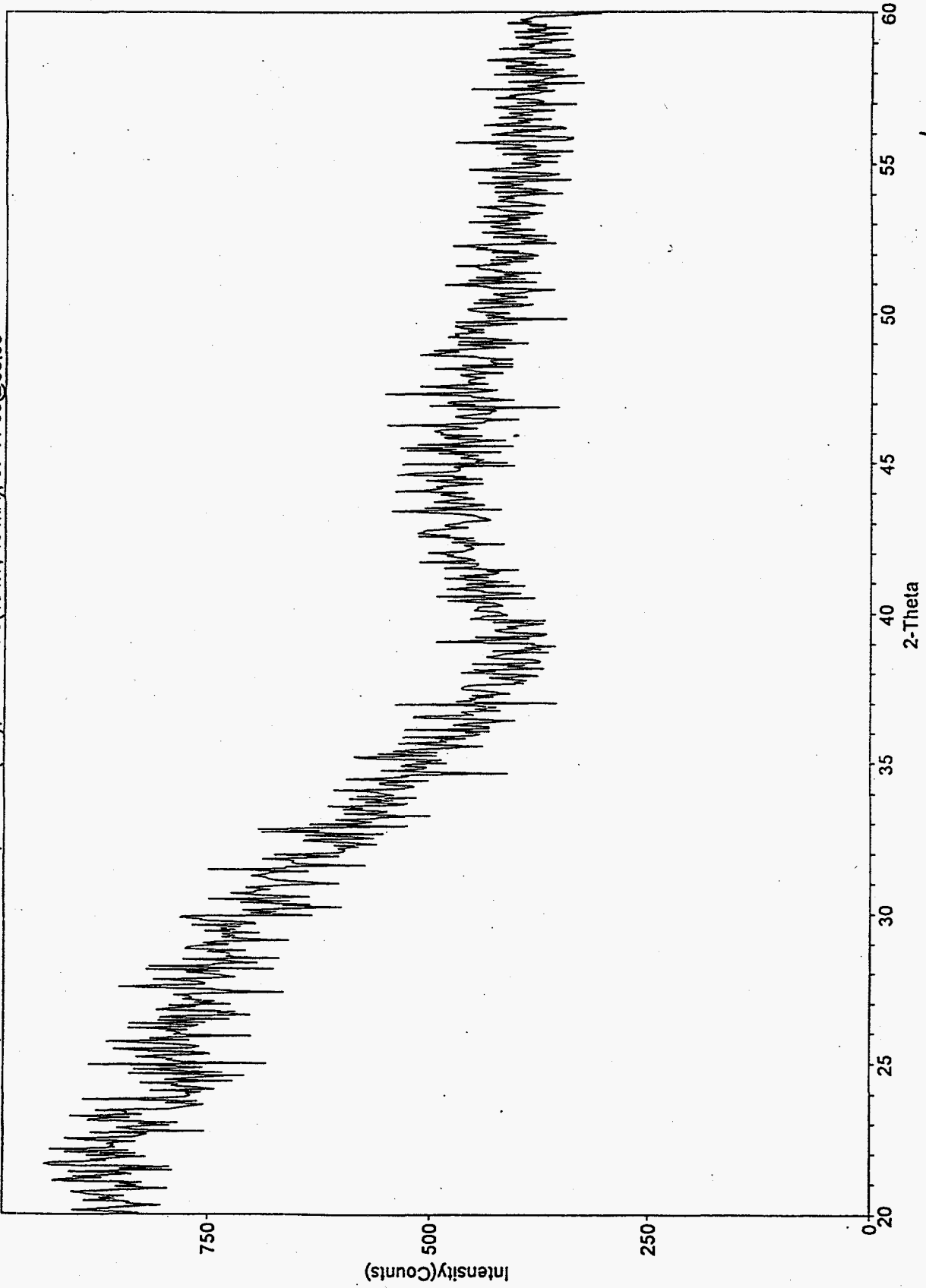


Figure 1. Raw XRD plot for sample V1, 20 to 60 degrees 2-theta.

<960718A.RD> V2 GLASS, Scan: 5.0-70.0/0.02, Dwell=20(sec), Anode=CU(45 kV, 40 mA), 07-19-96@07:48

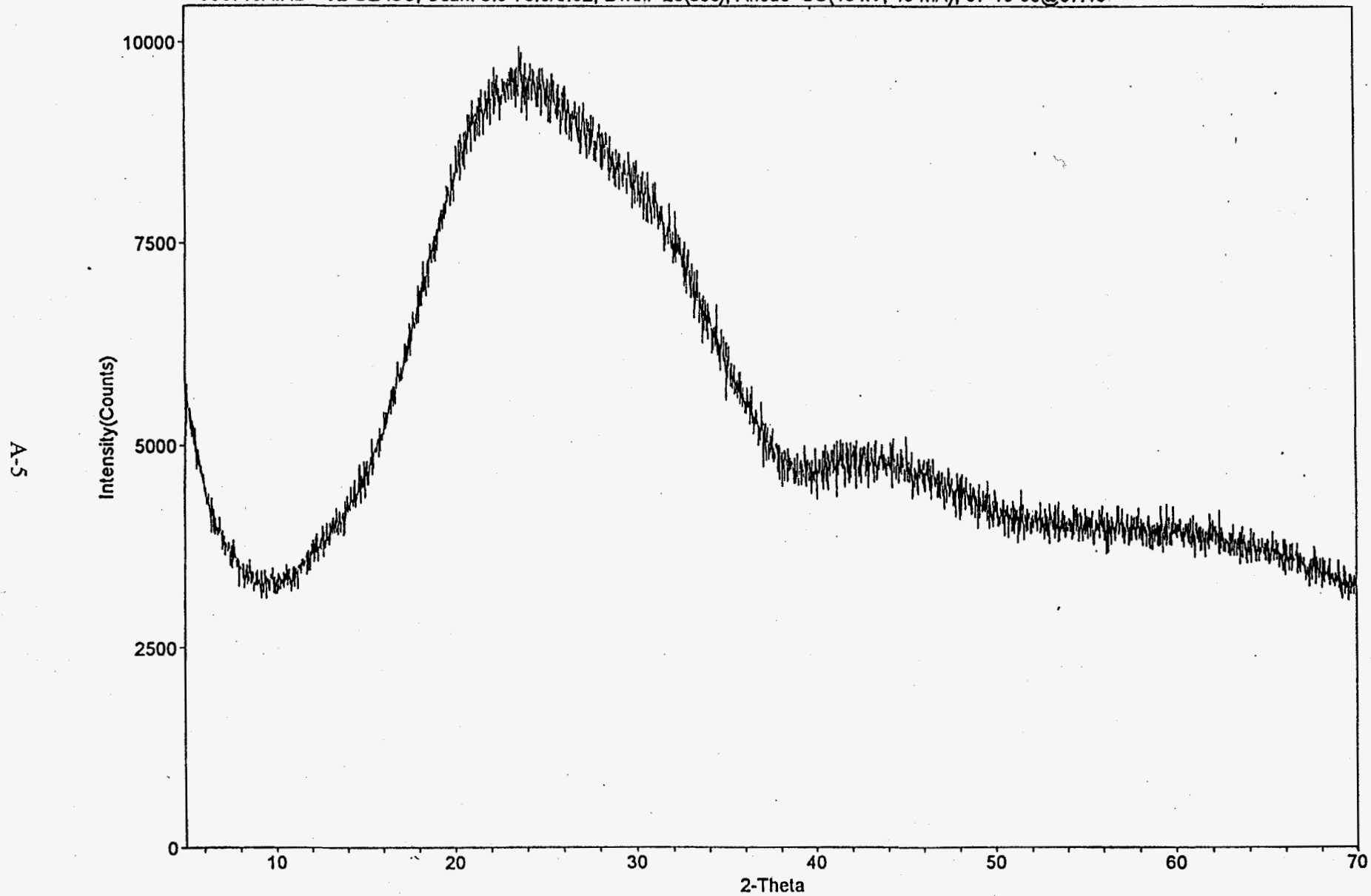


Figure 2. Raw XRD plot for sample V2, 5 to 70 degrees 2-theta.

<960722A.RD> V3, Scan: 5.0-75.0/0.05, Dwell=6(sec), Anode=CU(45 kV, 40 mA), 07-22-96(010:52

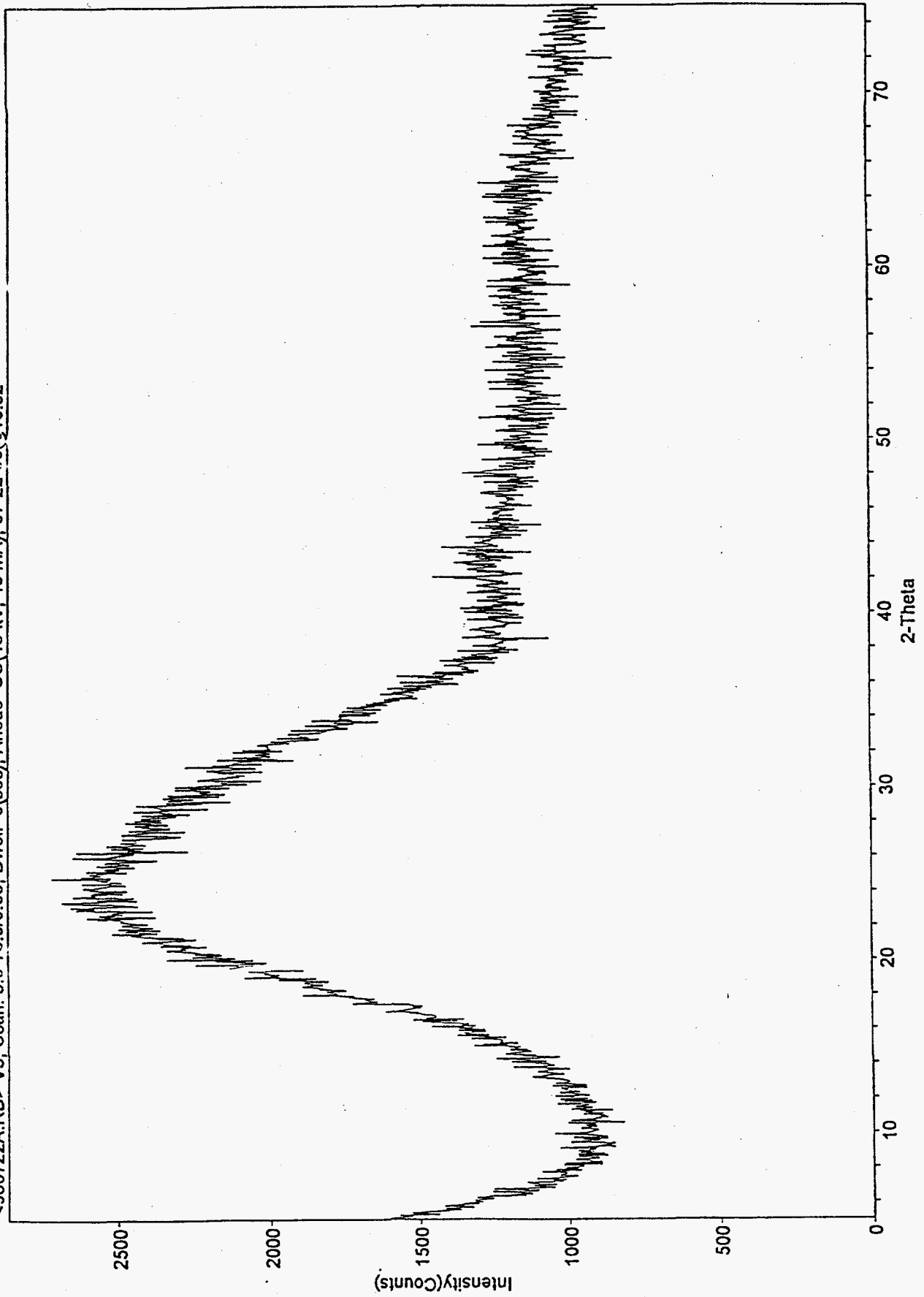


Figure 3. Raw XRD plot for sample V3, 5 to 75 degrees 2-theta.

<960723A.RD> V4, Scan: 5.0-75.0/0.05, Dwell=3(sec), Anode=CU(45 kV, 40 mA), 07-23-96@09:24

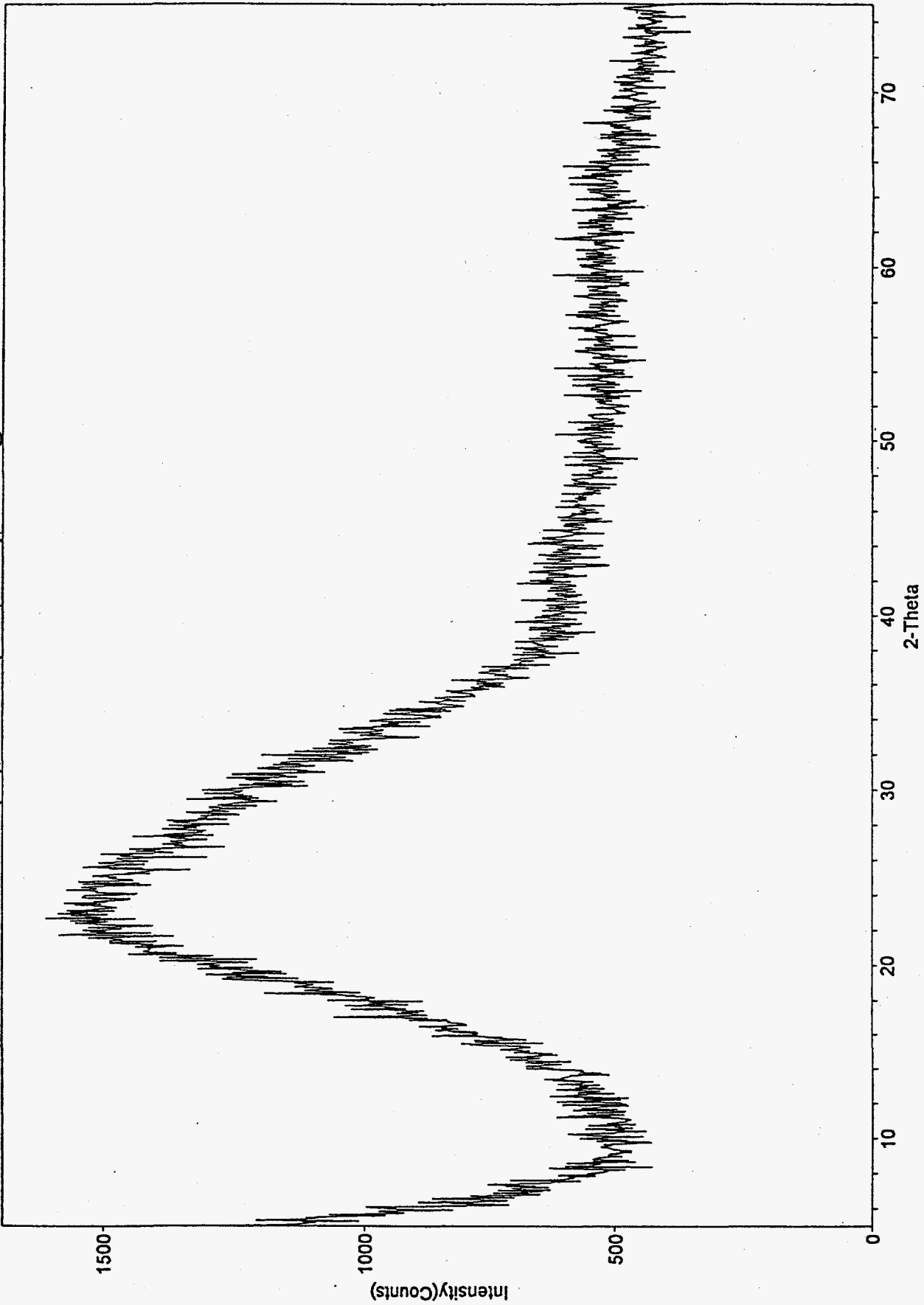


Figure 4. Raw XRD plot for sample V4, 5 to 75 degrees 2-theta.

<960731A.RD> V5, Scan: 5.0-75.0/0.05, Dwell=3(sec), Anode=CU(45 kV, 40 mA), 07-31-96@09:13

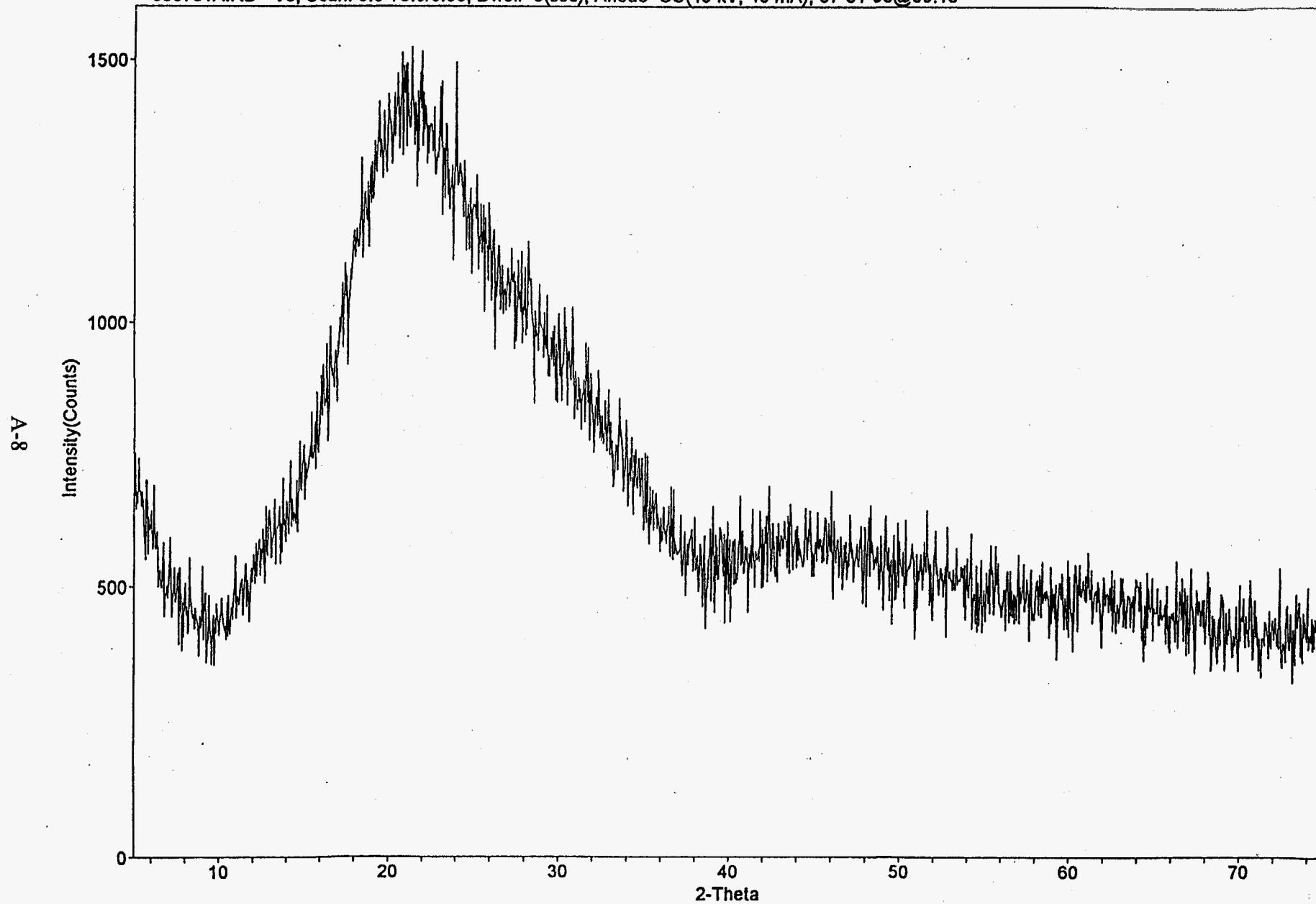


Figure 5. Raw XRD plot for sample V5, 5 to 75 degrees 2-theta.

<960730A.RD> V6, Scan: 5.0-75.0/0.05, Dwell=3(sec), Anode=CU(45 kV, 40 mA), 07-30-96@10:26

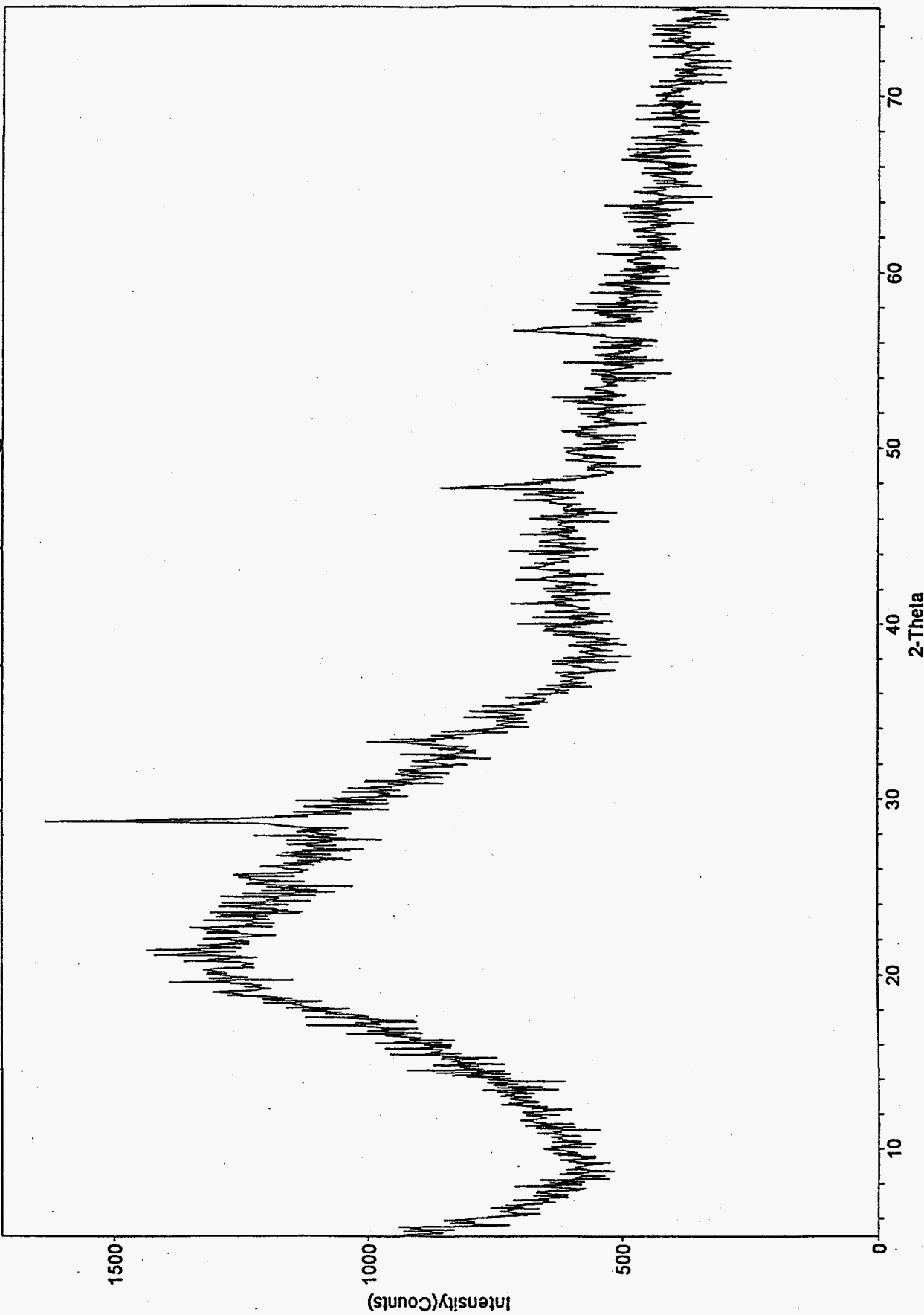


Figure 6. Raw XRD plot for sample V6, 5 to 75 degrees 2-theta.

<960801A.RD> V7, Scan: 5.0-75.0/0.05, Dwell=3(sec), Anode=Cu(45 kV, 40 mA), 08-01-96@11:28

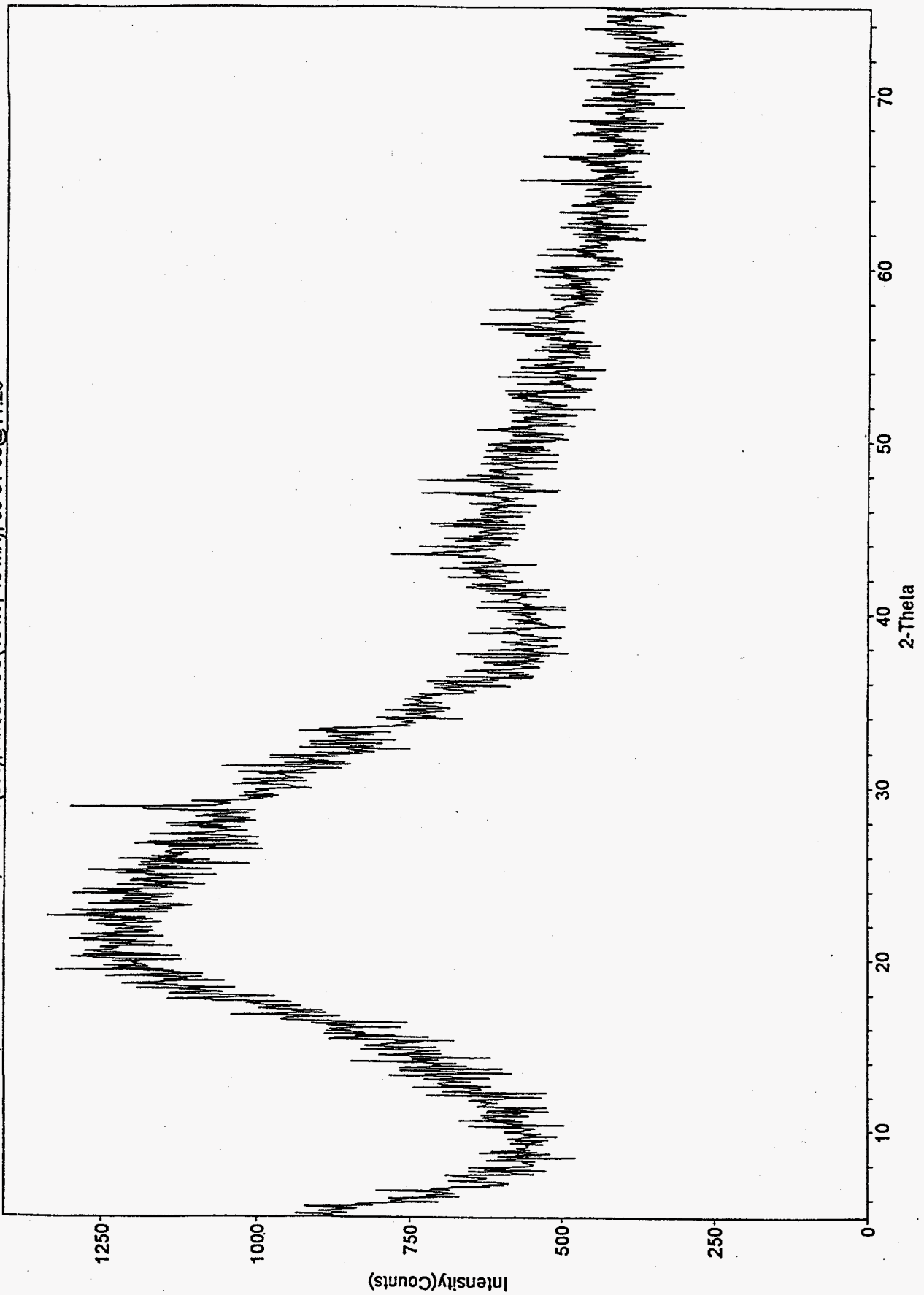


Figure 7. Raw XRD plot for sample V7, 5 to 75 degrees 2-theta.



<960711B.RD> V1, Scan: 25.0-35.0/0.02, Dwell=20(sec), Anode=CU(45 kV, 40 mA), 07-12-96@08:06

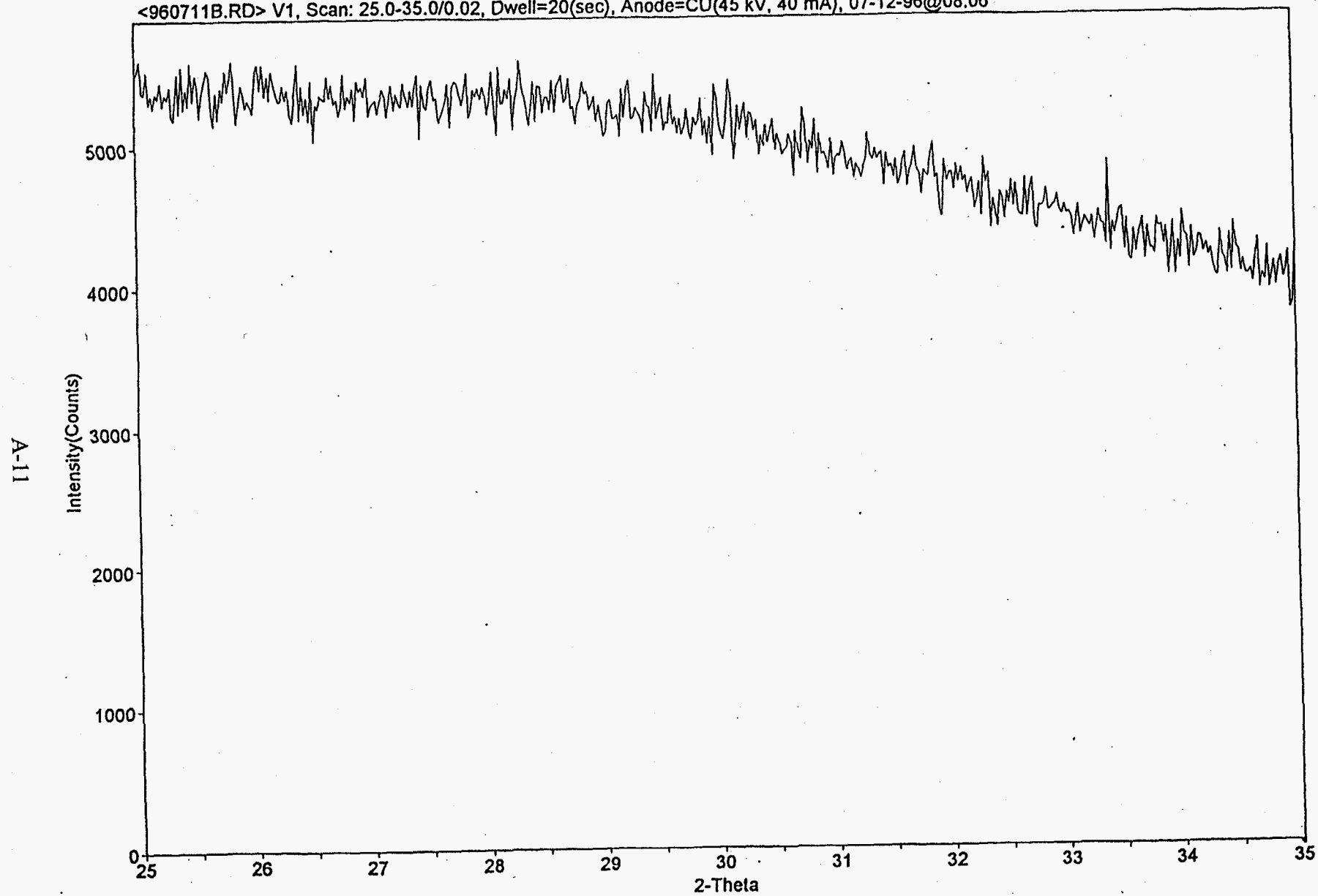


Figure 8. Raw XRD plot for sample V1, 25 to 35 degrees 2-theta.

<960806A.RD> V2, Scan: 25.0-35.0/0.02, Dwell=20(sec), Anode=CU(45 kV, 40 mA), 08-06-96@11:14

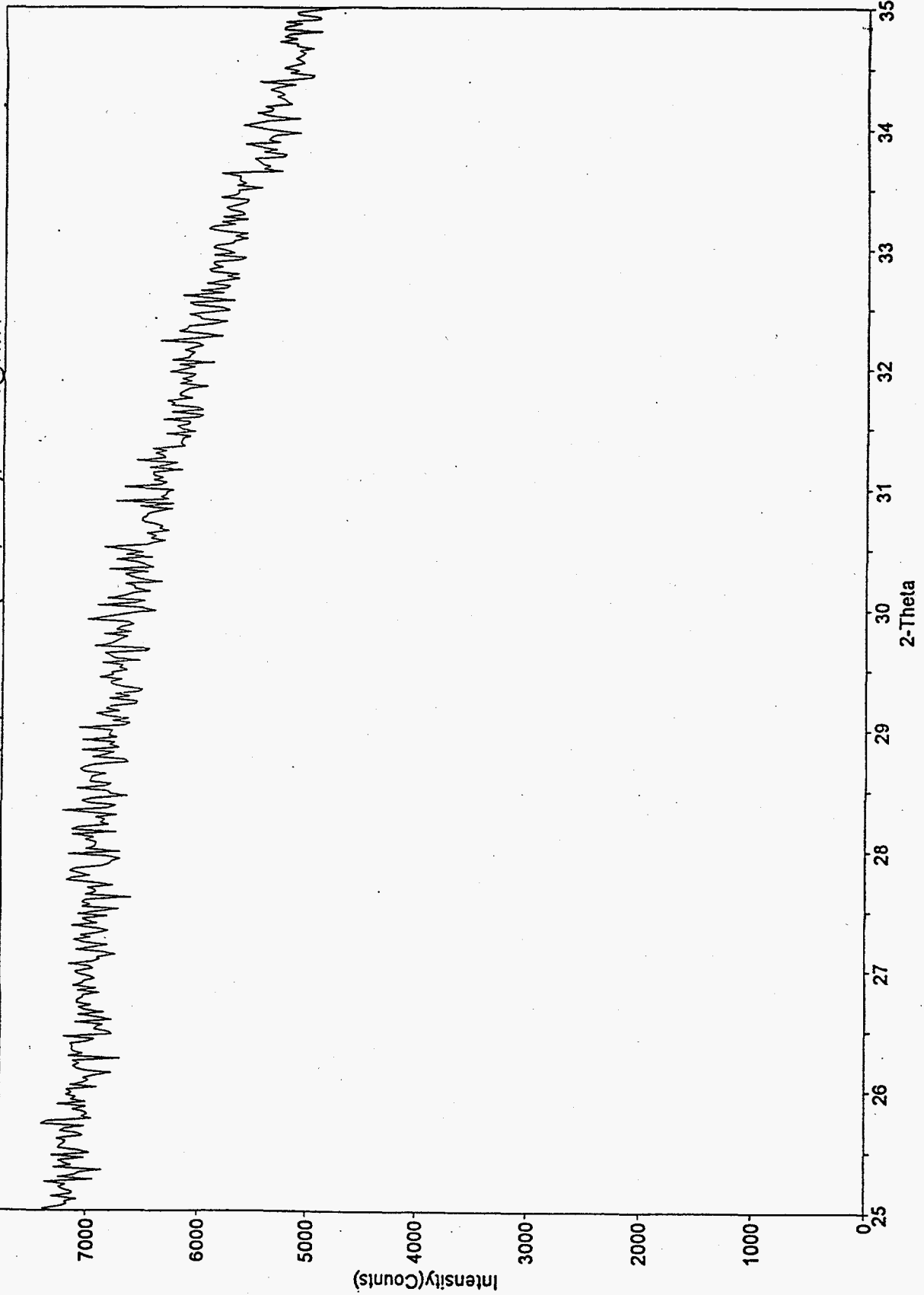


Figure 9. Raw XRD plot for sample V2, 25 to 35 degrees 2-theta.

<960722B.RD> V3, Scan: 25.0-35.0/0.02, Dwell=20(sec), Anode=CU(45 kV, 40 mA), 07-23-96@07:45

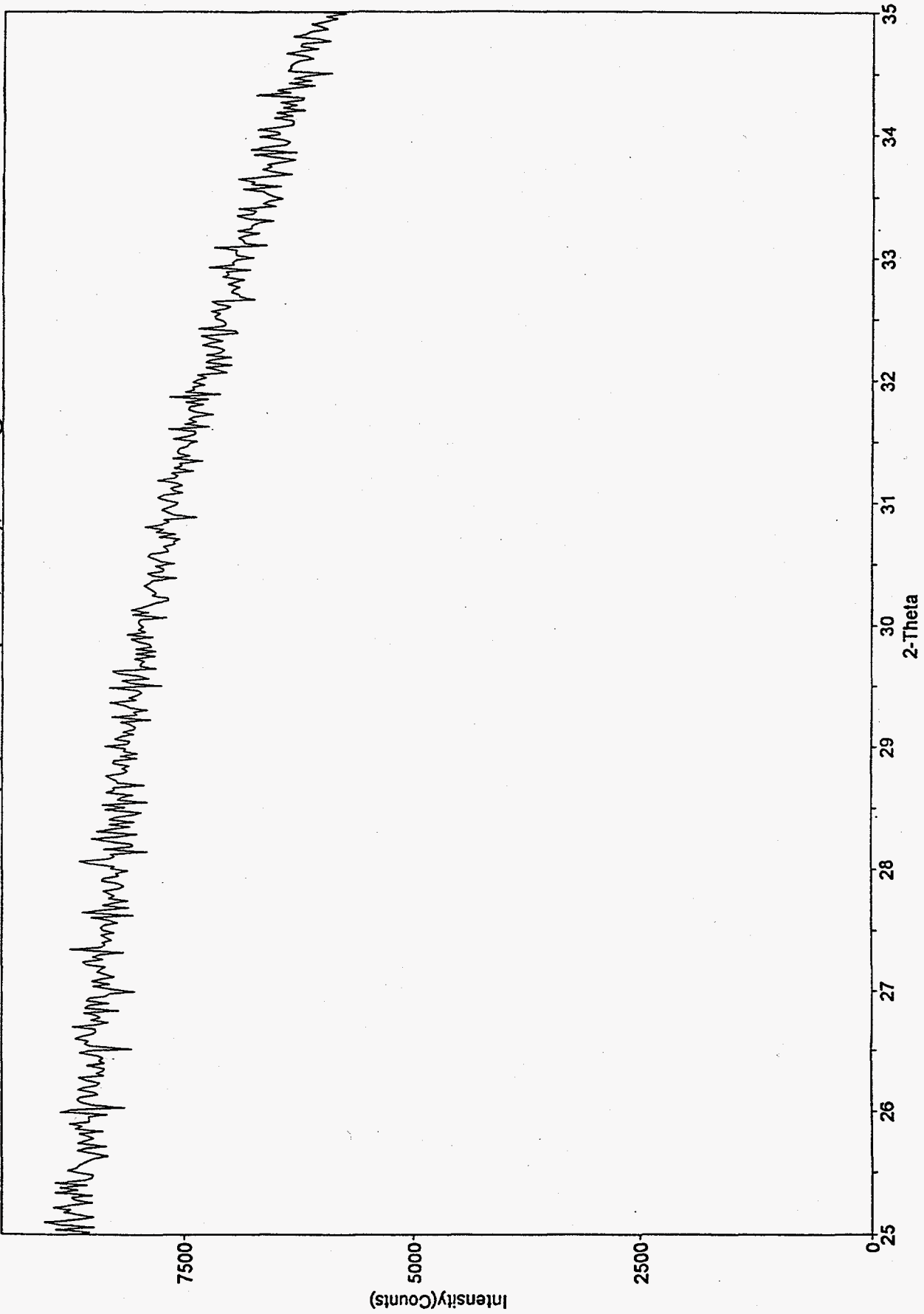


Figure 10. Raw XRD plot for sample V3, 25 to 35 degrees 2-theta.

<960802B.RD> V4, Scan: 25.0-35.0/0.02, Dwell=20(sec), Anode=CU(45 kV, 40 mA), 08-14-96@08:11

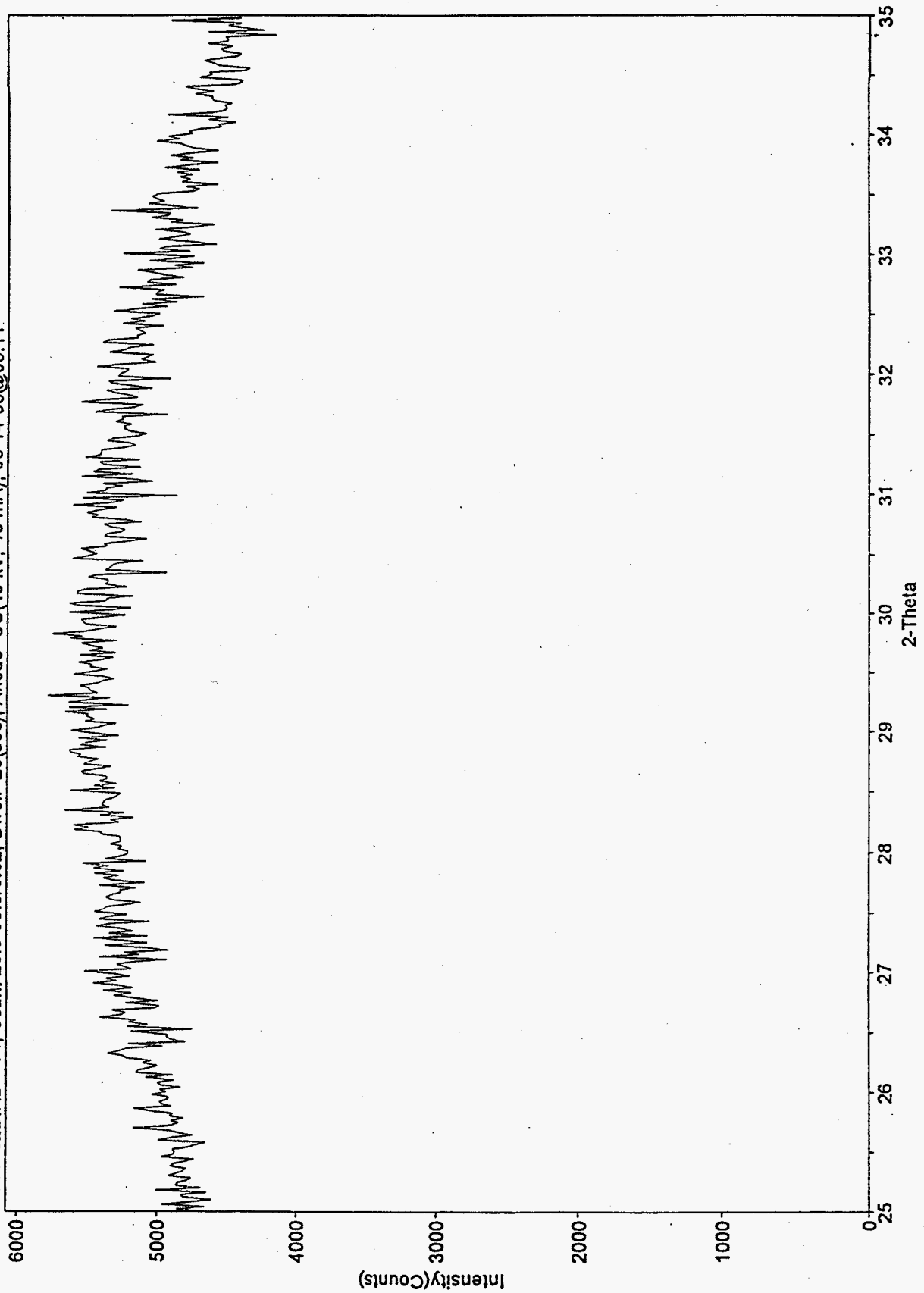


Figure 11. Raw XRD plot for sample V4, 25 to 35 degrees 2-theta.

<960731B.RD> V5, Scan: 25.0-35.0/0.02, Dwell=20(sec), Anode=CU(45 kV, 40 mA), 08-01-96@09:07

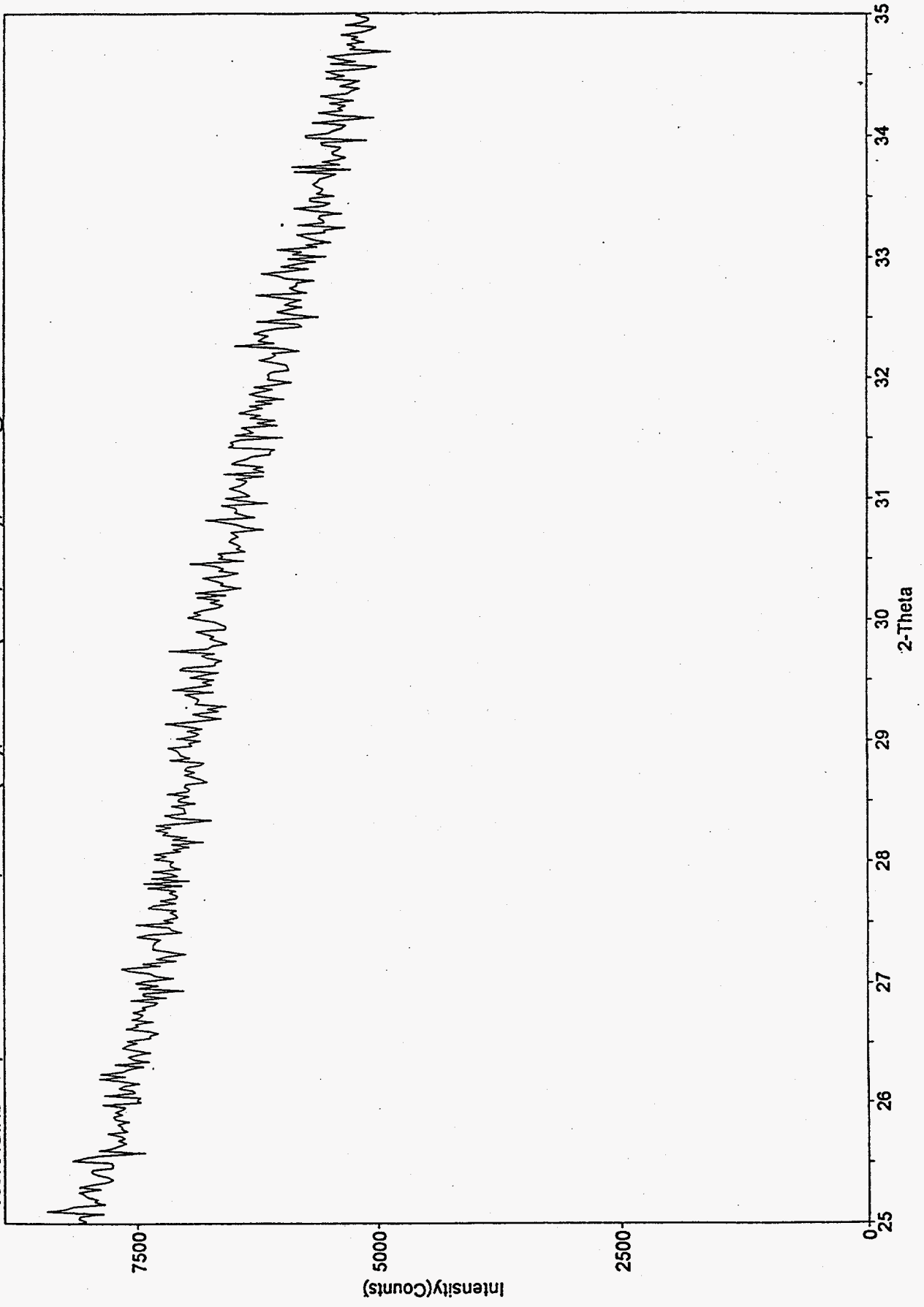


Figure 12. Raw XRD plot for sample V5, 25 to 35 degrees 2-theta.

<960730B.RD> V6, Scan: 25.0-35.0/0.02, Dwell=20(sec), Anode=CU(45 kV, 40 mA), 07-31-96@07.42

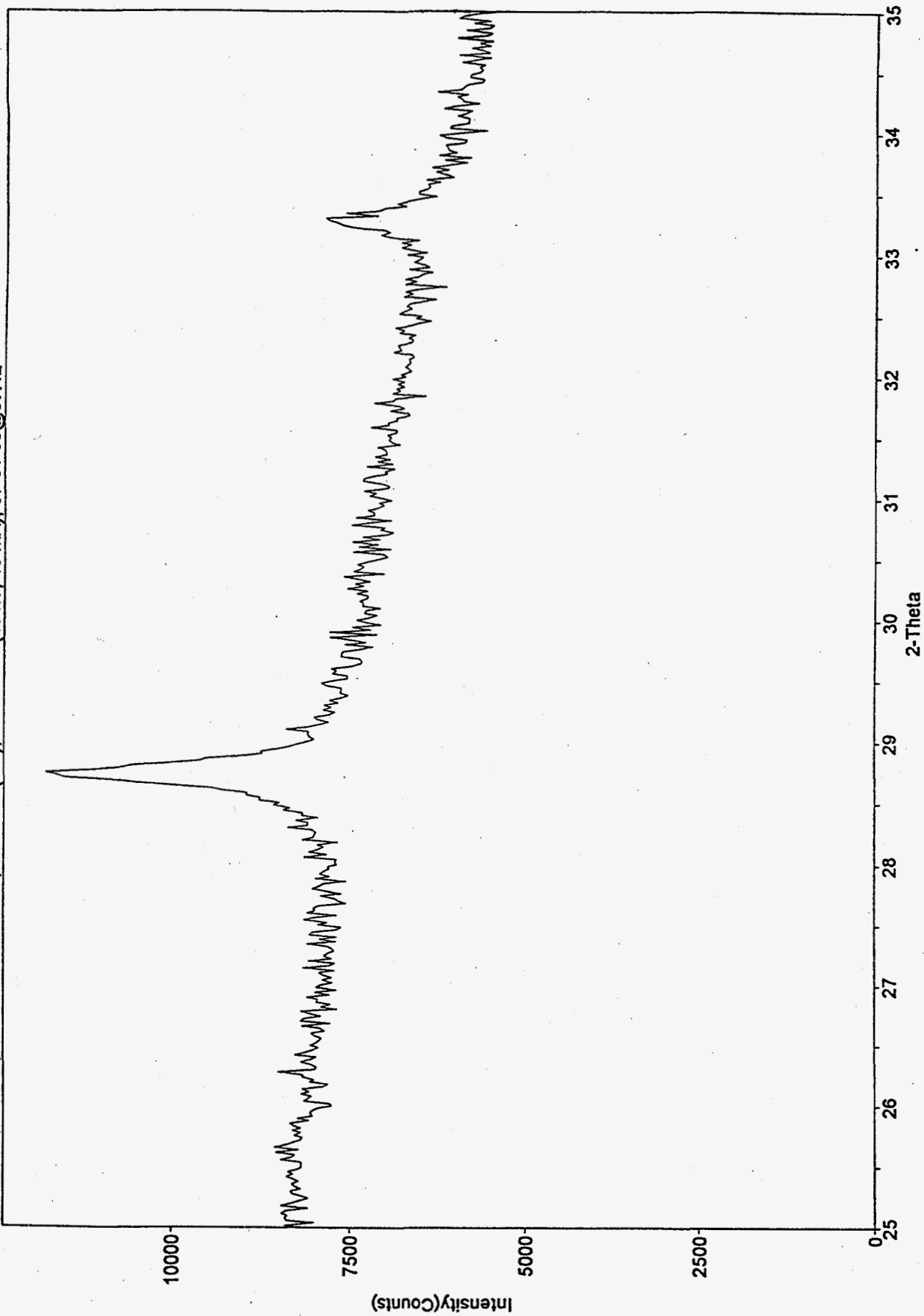


Figure 13. Raw XRD plot for sample V6, 25 to 35 degrees 2-theta.

<960801B.RD> V7, Scani: 25.0-35.0/0.02, Dwell=20(sec), Anode=CuJ(45 kV, 40 mA), 08-02-96@07:55

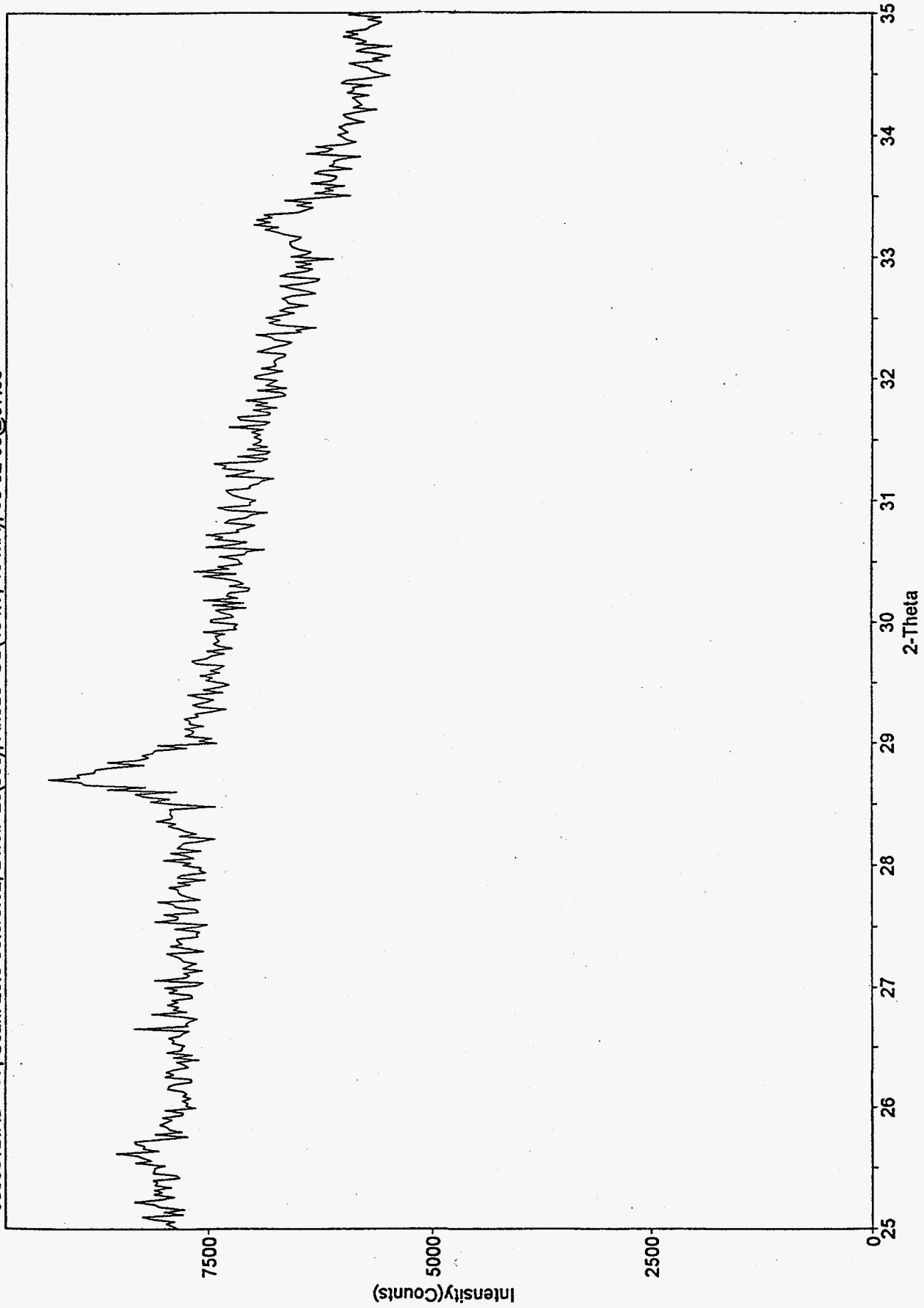


Figure 14. Raw XRD plot for sample V7, 25 to 35 degrees 2-theta.

<960711A.DIF> V1, Scan: 20.0-60.0/0.05, Dwell=3(sec), Anode=CU(45 kV, 40 mA), 07-11-96@09:21

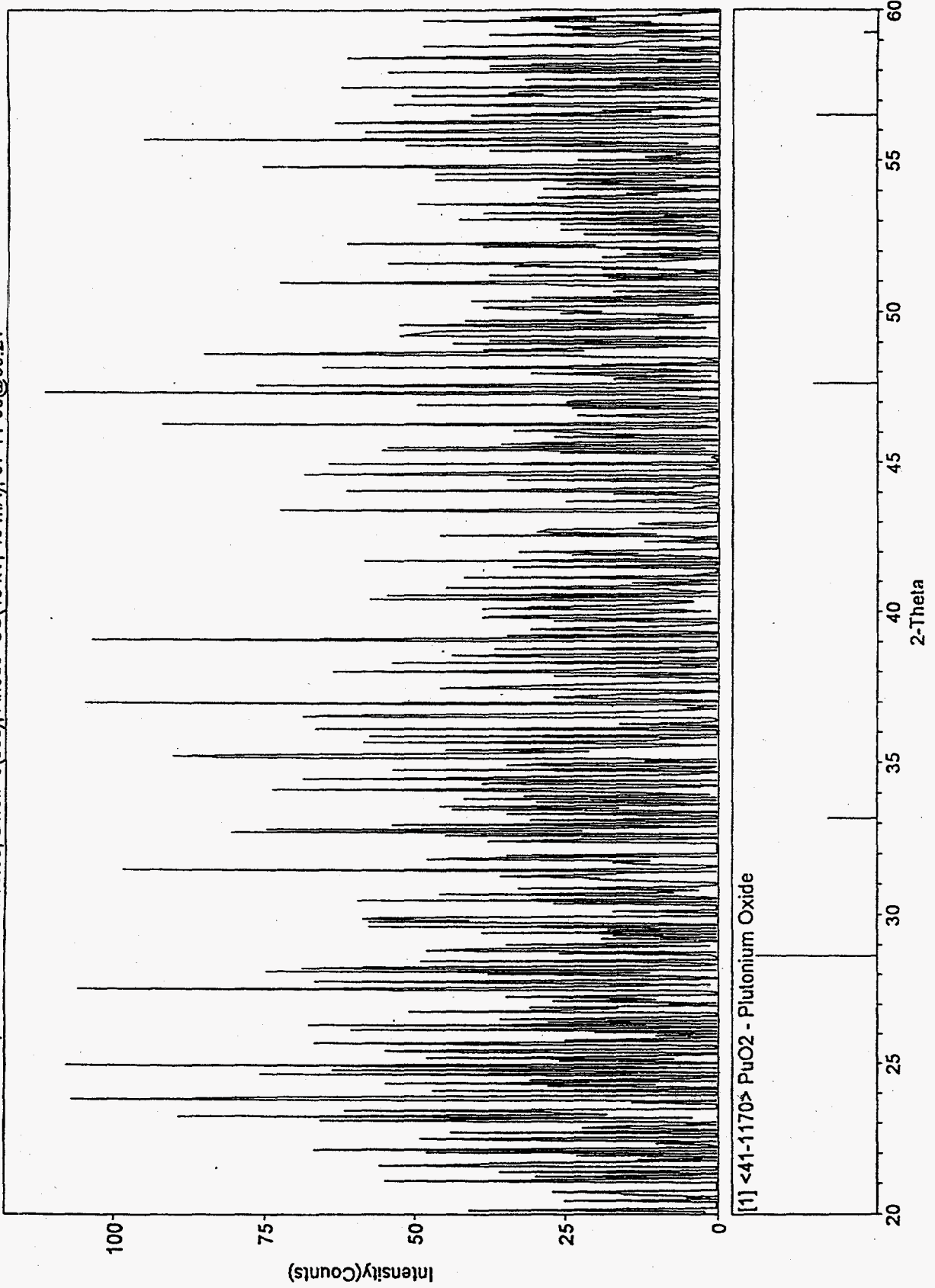
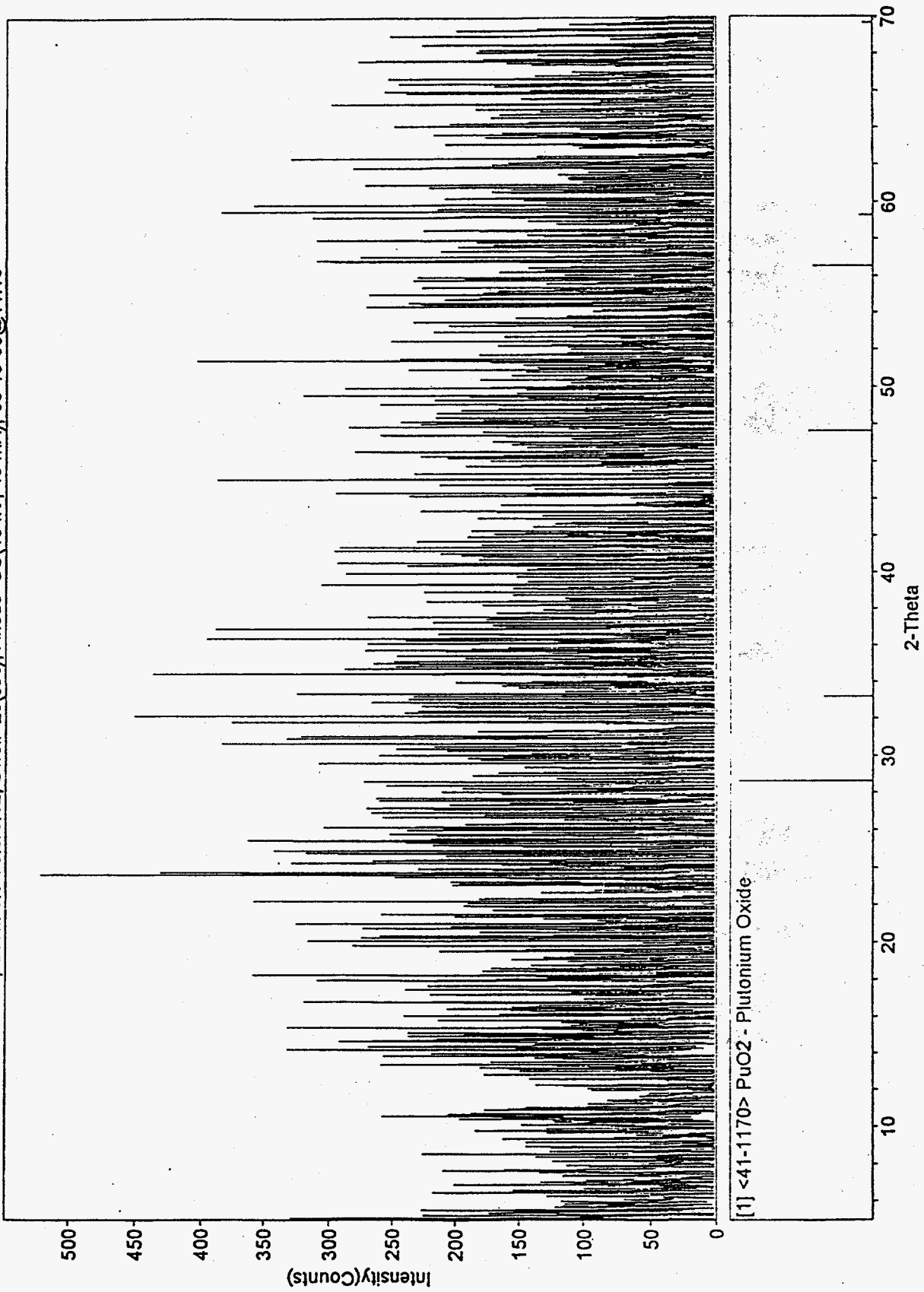


Figure 15. Background subtracted XRD plot for sample V1, 20 to 60 degrees 2-theta. "Stick Figure" display of PuO<sub>2</sub> pattern shown.



<960718A.DIF> V2 GLASS, Scan: 5.0-70.0/0.02, Dwell=20(sec), Anode=Cu(45 kV, 40 mA), 08-13-96@11:10



[1] <41-1170> PuO2 - Plutonium Oxide

Figure 16. Background subtracted XRD plot for sample V2, 5 to 70 degrees 2-theta. "Stick Figure" display of PuO<sub>2</sub> pattern shown.

<960722A.DIF> V3, Scan: 5.0-75.0/0.05, Dwell=6(sec), Anode=CU(45 kV, 40 mA), 07-22-96@10:57

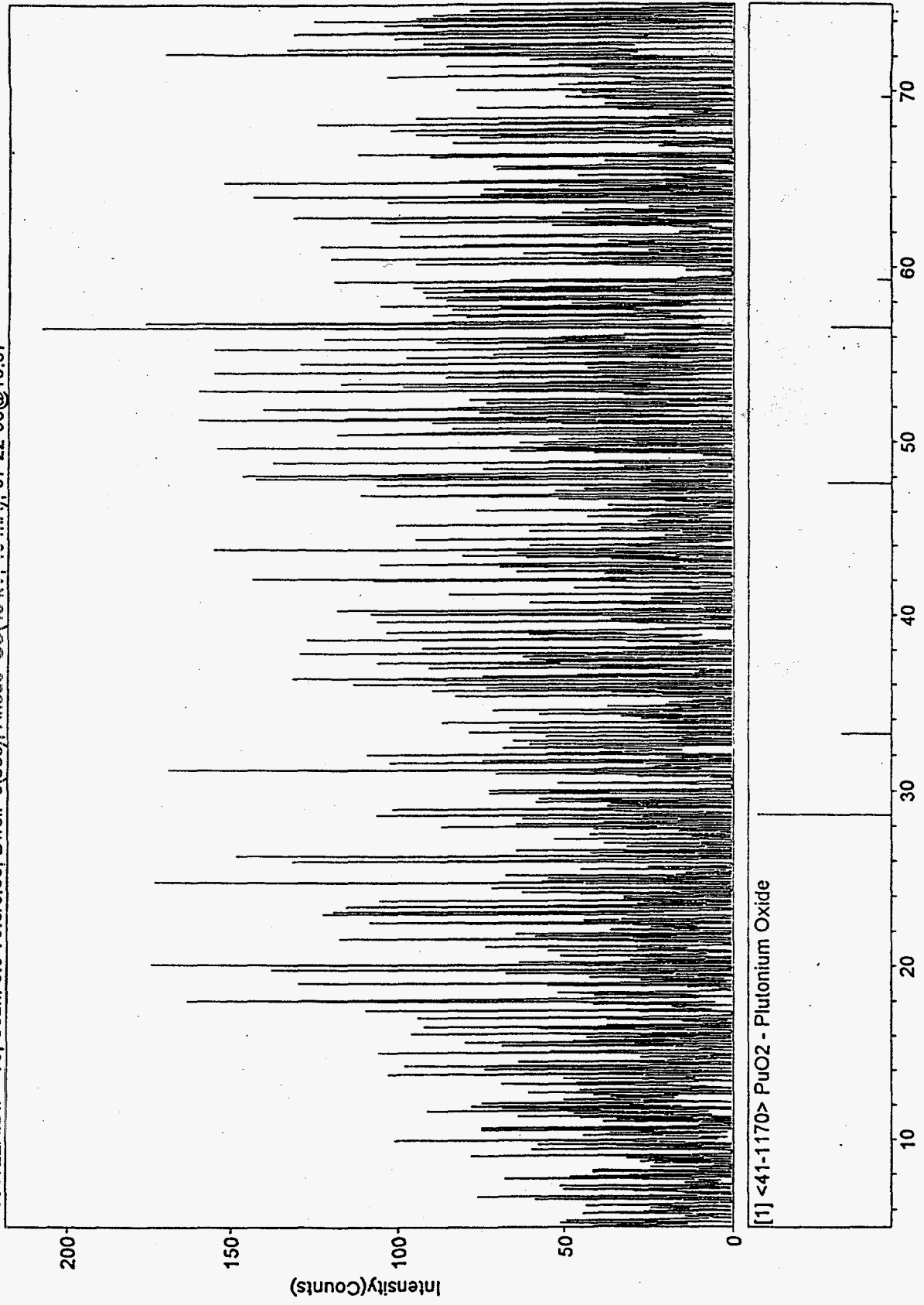


Figure 17. Background subtracted XRD plot for sample V3, 5 to 75 degrees 2-theta. "Stick Figure" display of PuO<sub>2</sub> pattern shown.

<960723A.DIF> V4, Scan: 5.0-75.0/0.05, Dwell=3(sec), Anode=CU(45 kV, 40 mA), 07-23-96@09:28

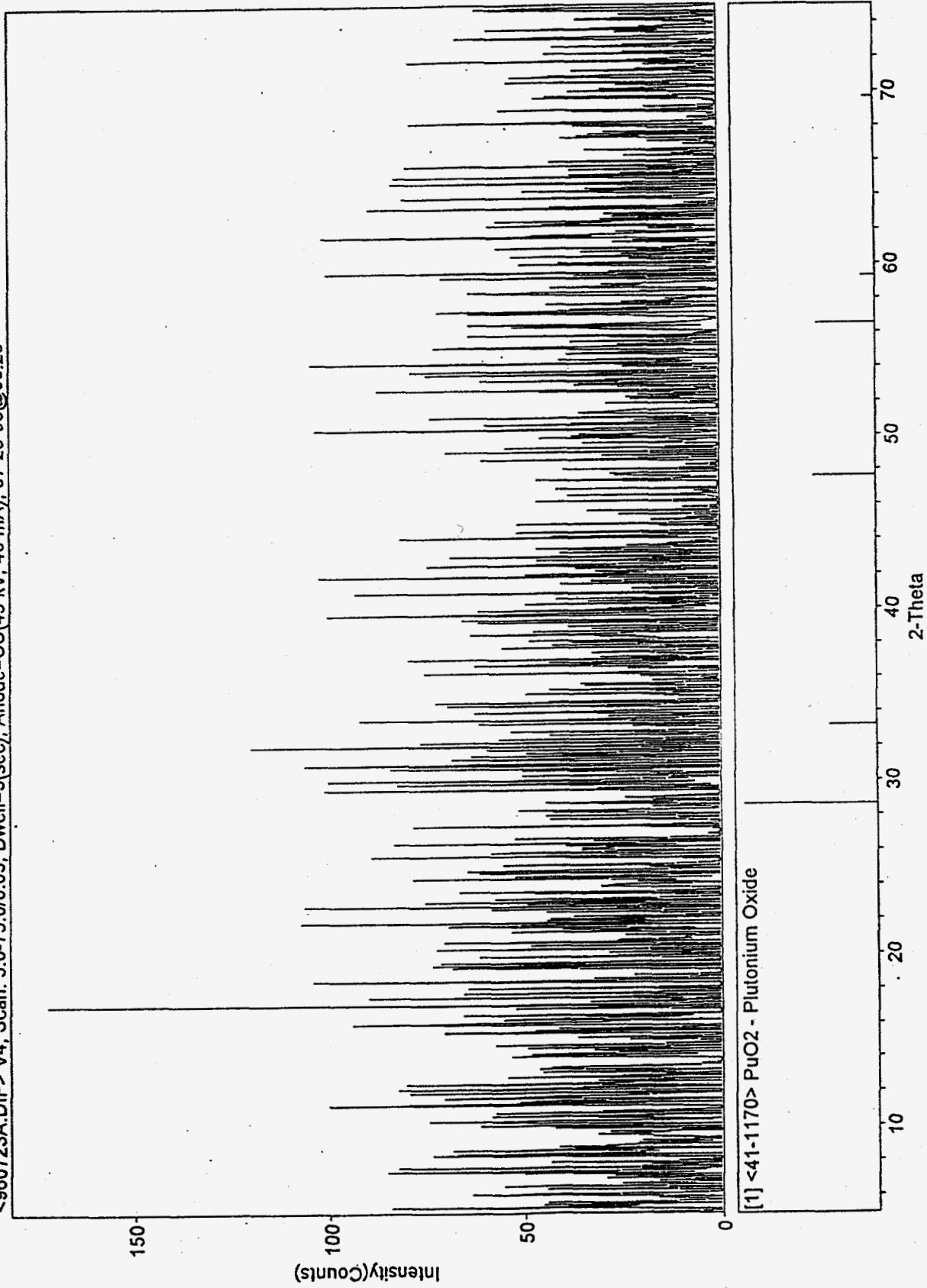


Figure 18. Background subtracted XRD plot for sample V4, 5 to 75 degrees 2-theta. "Stick Figure" display of PuO<sub>2</sub> pattern shown.

<960731A.DIF> V5, Scan: 5.0-75.0/0.05, Dwell=3(sec), Anode=Cu(45 kV, 40 mA), 08-01-96@09:40

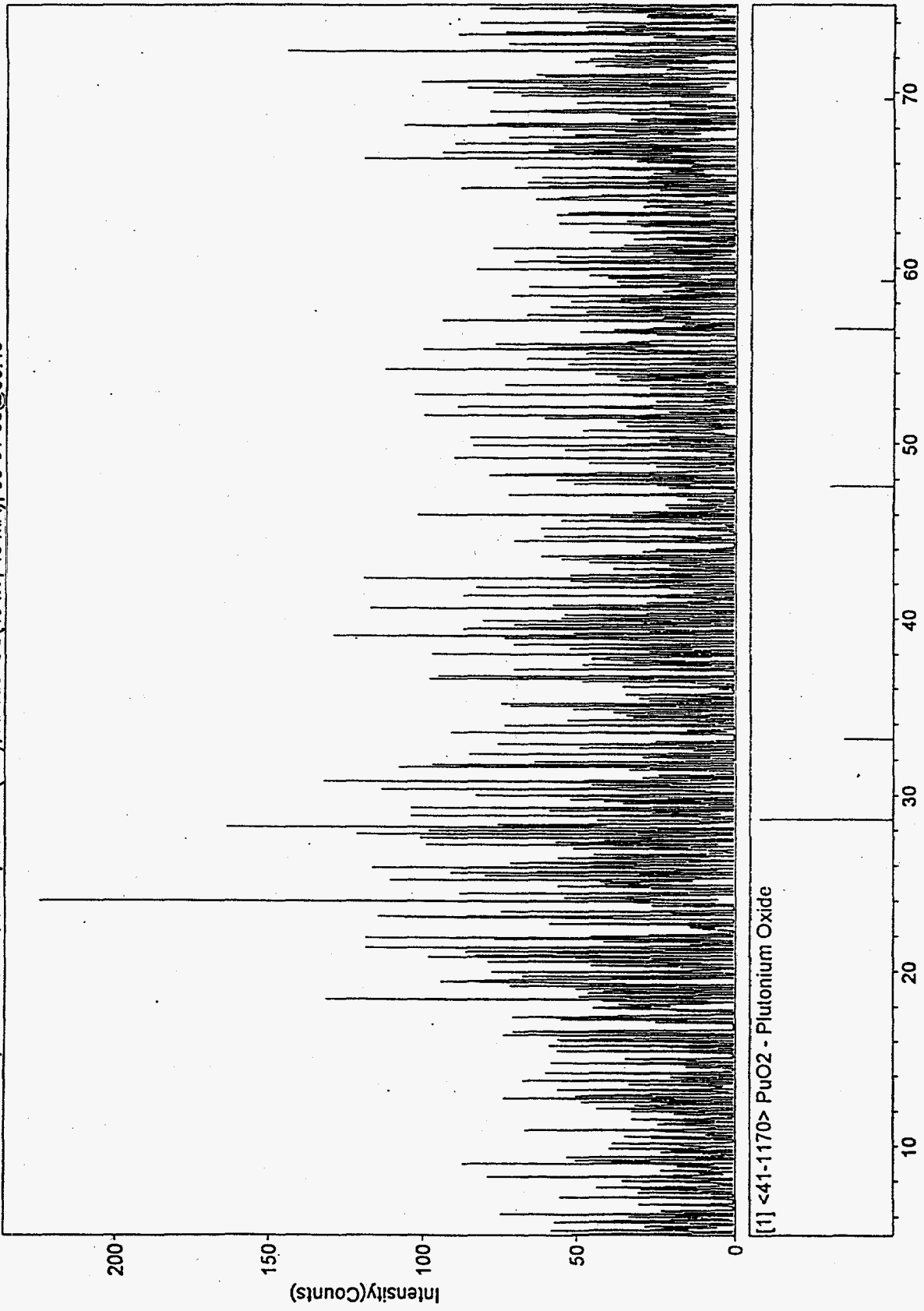


Figure 19. Background subtracted XRD plot for sample V5, 5 to 75 degrees 2-theta. "Stick Figure" display of PuO<sub>2</sub> pattern shown.

<960730A.DIF> V6, Scan: 5.0-75.0/0.05, Dwell=3(sec), Anode=CU(45 kV, 40 mA), 07-30-96@10:31

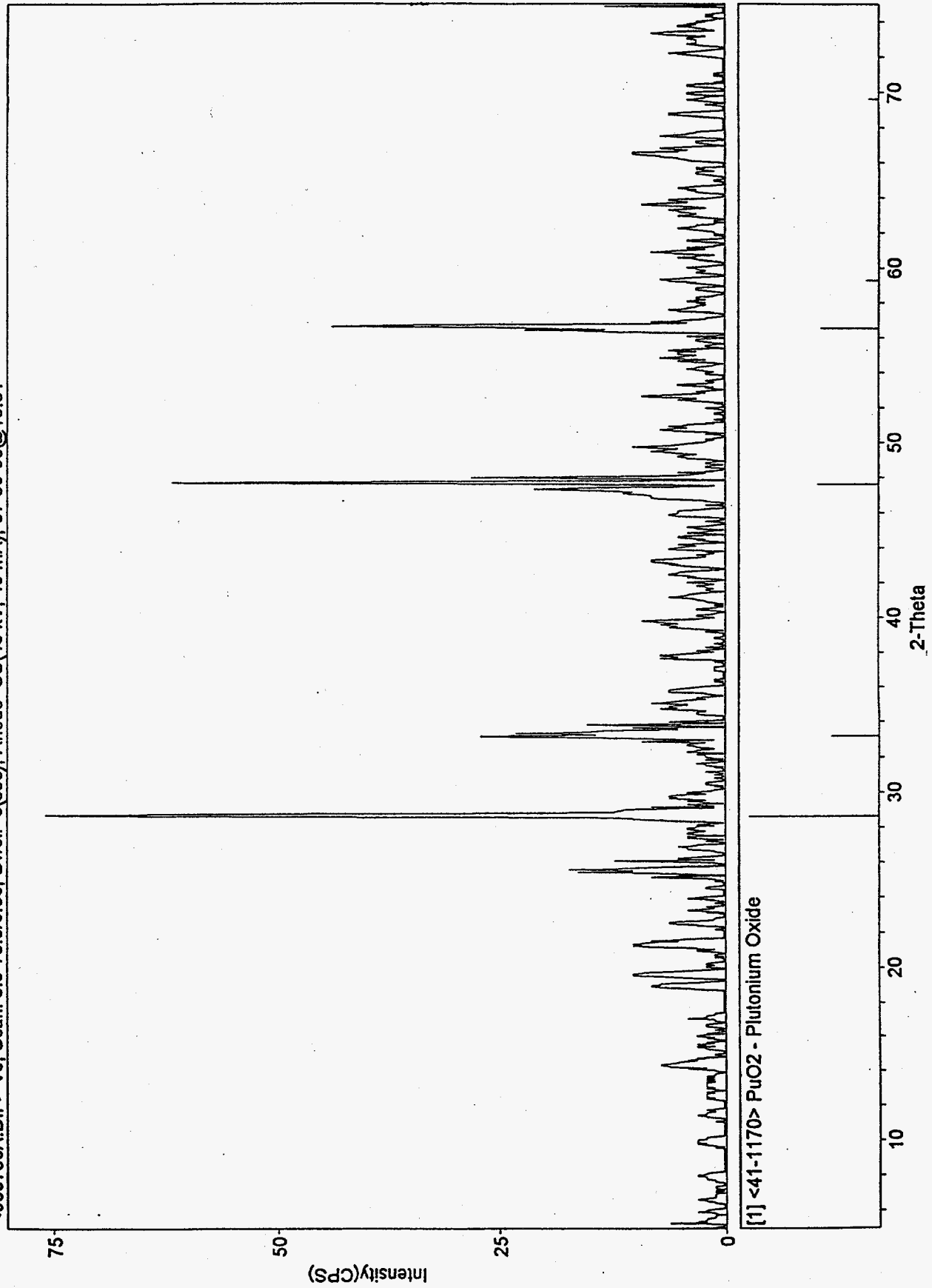


Figure 20. Background subtracted XRD plot for sample V6, 5 to 75 degrees 2-theta. "Stick Figure" display of PuO<sub>2</sub> pattern shown.

<960801A.DIF> V7, Scan: 5.0-75.0/0.05, Dwell=3(sec), Anode=CU(45 kV, 40 mA), 08-01-96@11:32

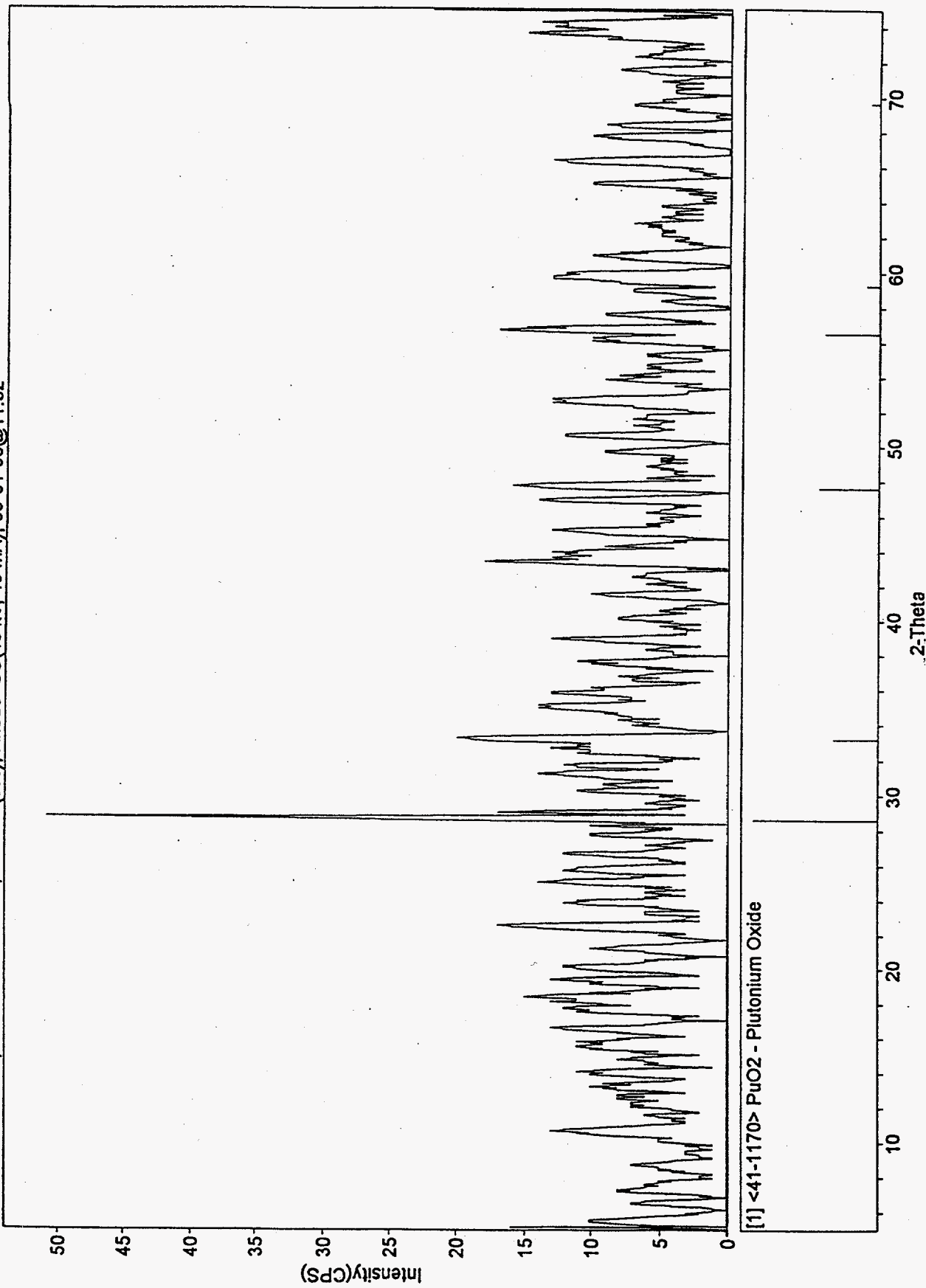


Figure 21. Background subtracted XRD plot for sample V7, 5 to 75 degrees 2-theta. "Stick Figure" display of PuO<sub>2</sub> pattern shown.

<960711B.DIF> V1, Scan: 25.0-35.0/0.02, Dwell=20(sec), Anode=CU(45 kV, 40 mA), 07-12-96@08:08

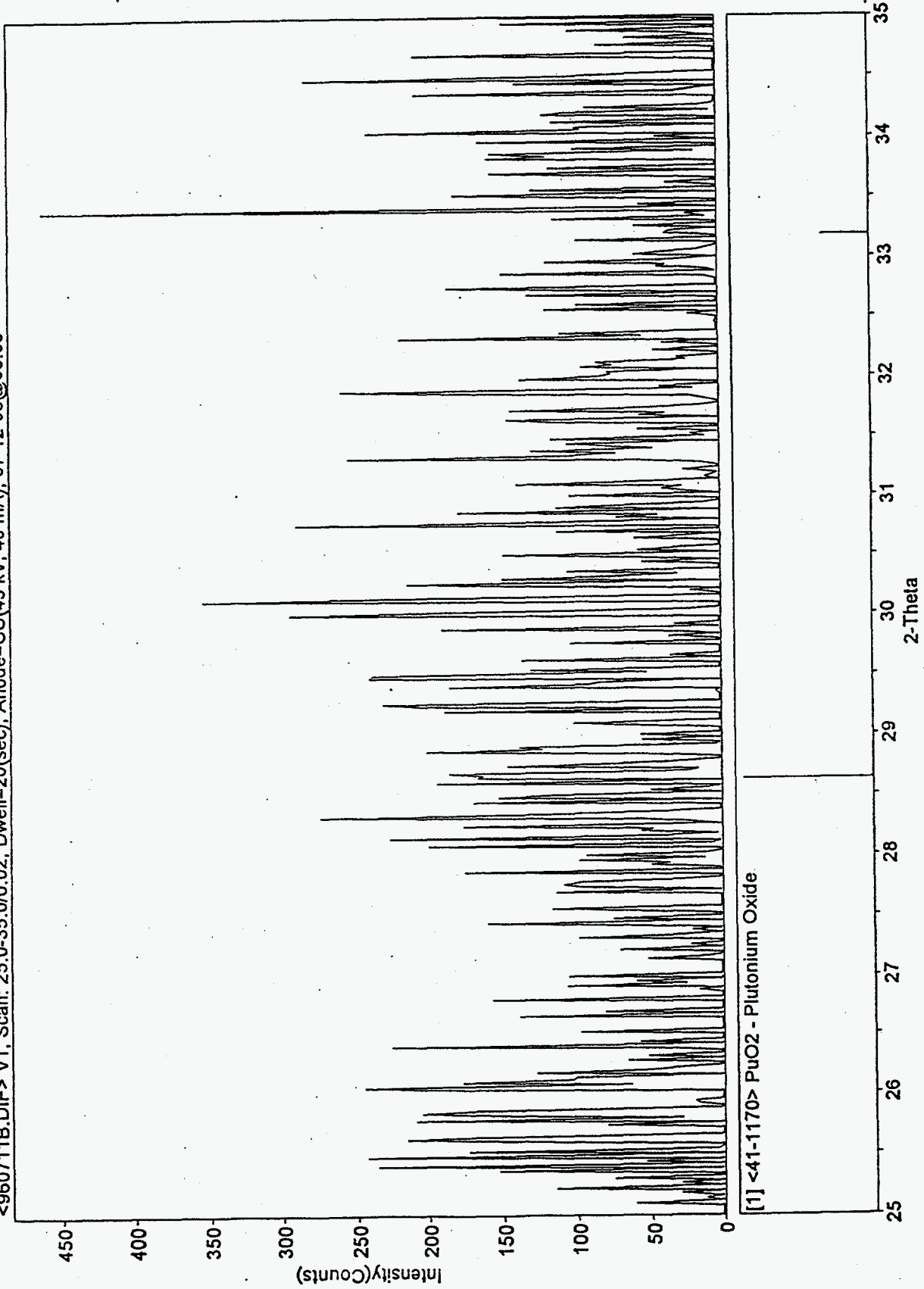


Figure 22. Background subtracted XRD plot for sample V1, 25 to 35 degrees 2-theta. "Stick Figure" display of PuO<sub>2</sub> pattern shown.

<960806A.DIF> V2, Scan: 25.0-35.0/0.02, Dwell=20(sec), Anode=CU(45 kV, 40 mA), 08-13-96@11:17

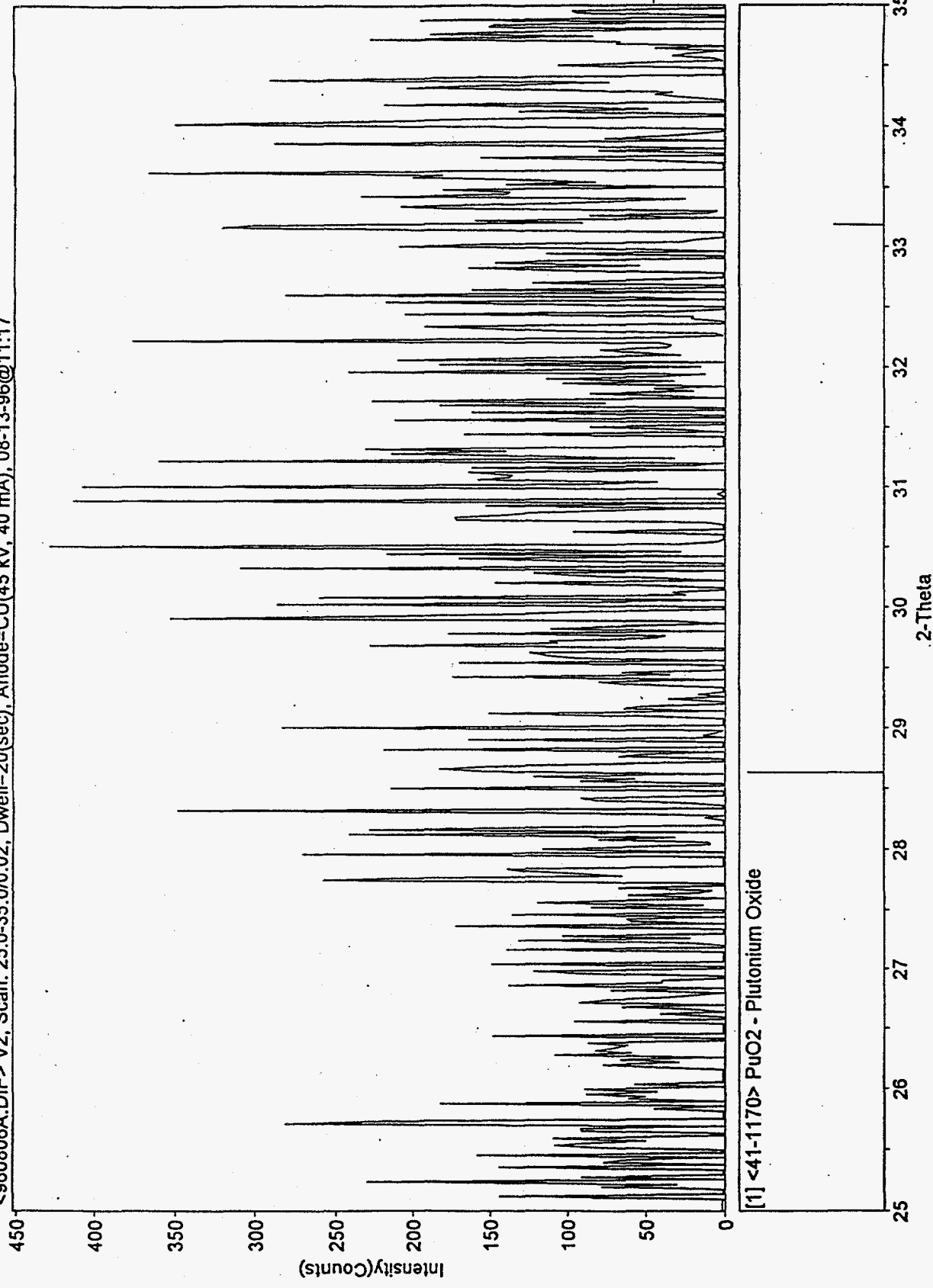


Figure 23. Background subtracted XRD plot for sample V2, 25 to 35 degrees 2-theta. "Stick Figure" display of PuO<sub>2</sub> pattern shown.



<960722B.DIF> V3, Scan: 25.0-35.0/0.02, Dwell=20(sec), Anode=CU(45 kV, 40 mA), 07-23-96@07:47

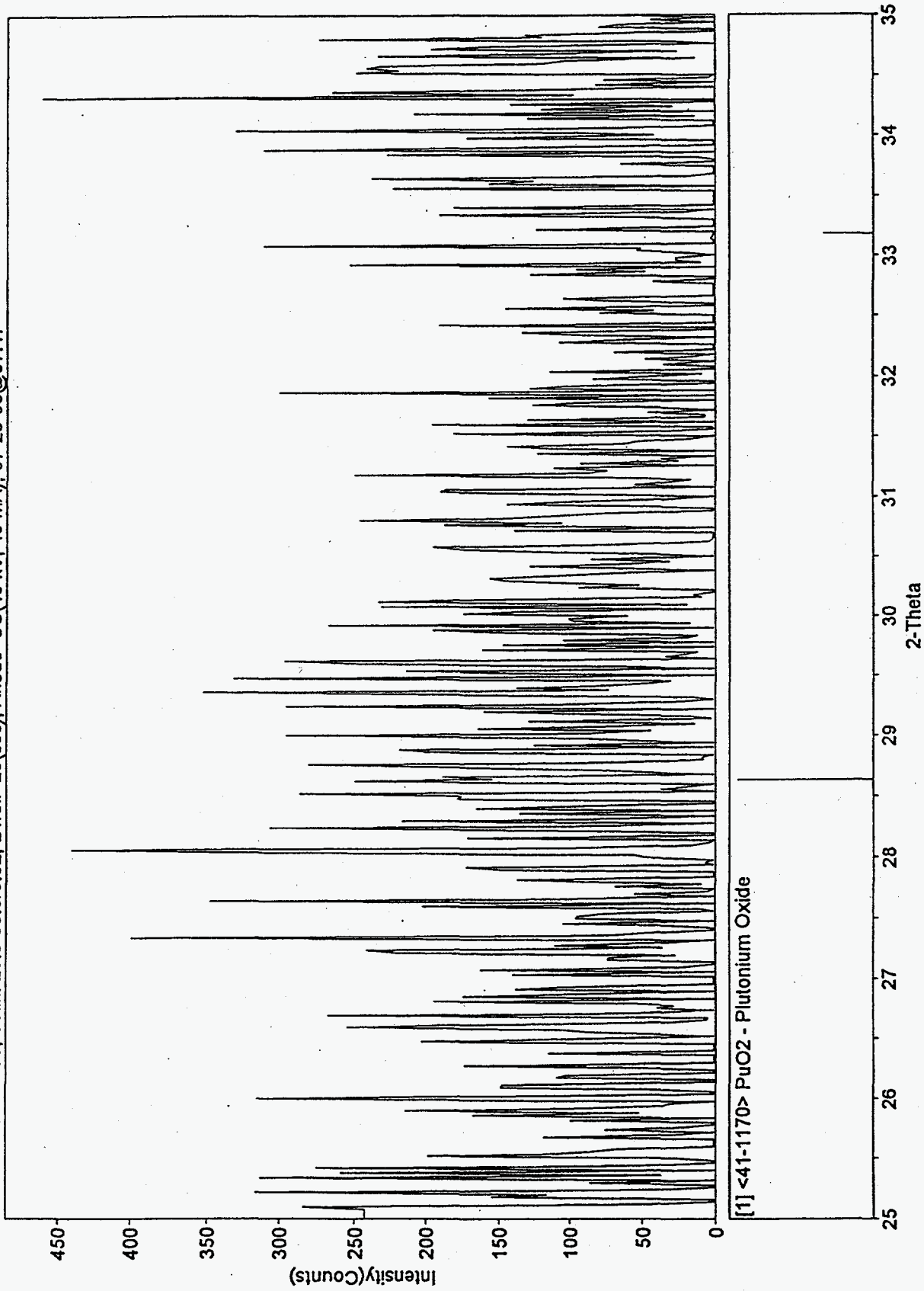


Figure 24. Background subtracted XRD plot for sample V3, 25 to 35 degrees 2-theta. "Stick Figure" display of PuO<sub>2</sub> pattern shown.

<960802B.DIF> V4, Scan: 25.0-35.0/0.02, Dwell=20(sec), Anode=CU(45 kV, 40 mA), 08-14-96@08:15

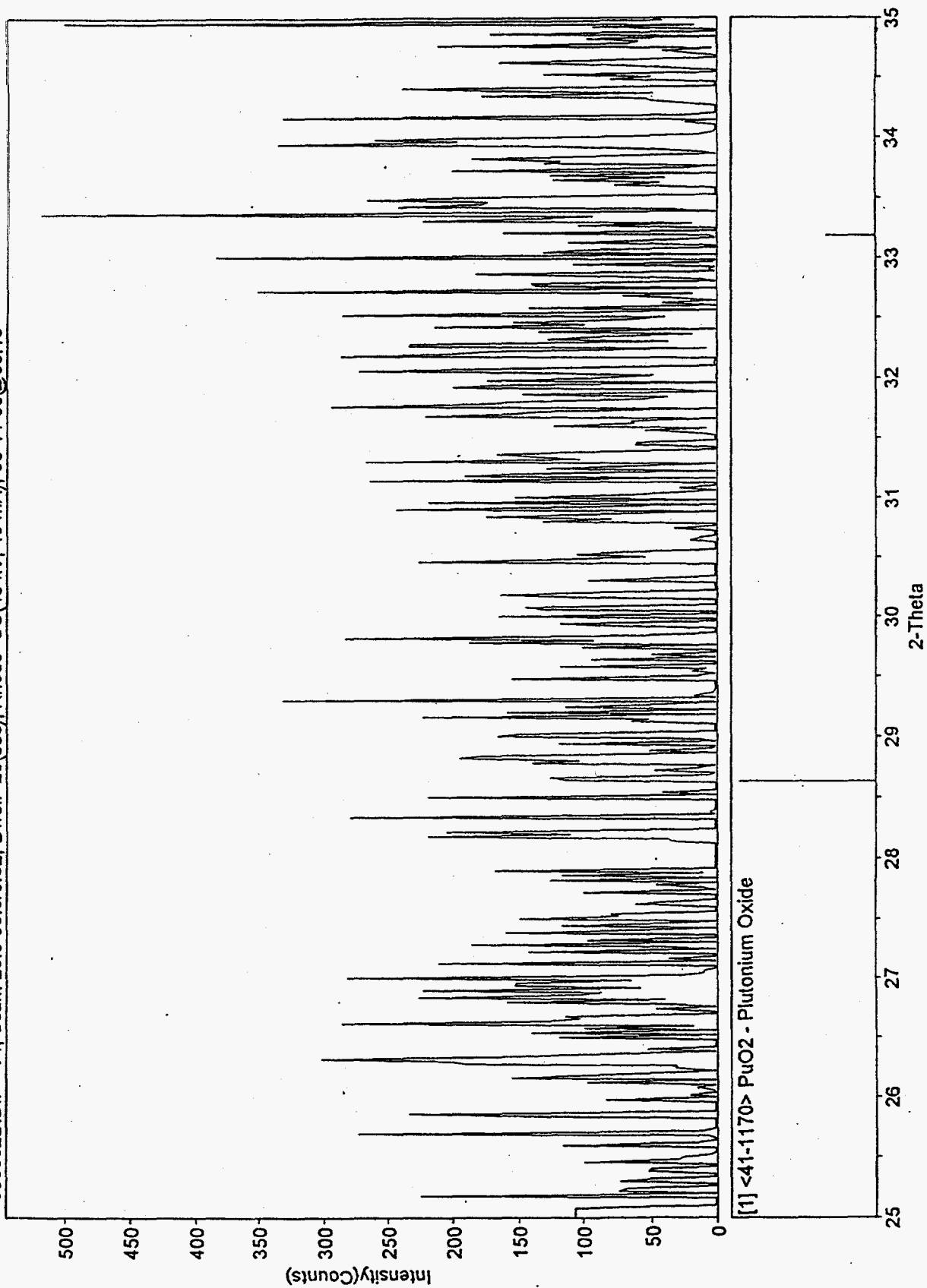


Figure 25. Background subtracted XRD plot for sample V4, 25 to 35 degrees 2-theta. "Stick Figure" display of PuO<sub>2</sub> pattern shown.

<960731B.DIF> V5, Scan: 25.0-35.0/0.02, Dwell=20(sec), Anode=CU(45 kV, 40 mA), 08-01-96@09:09

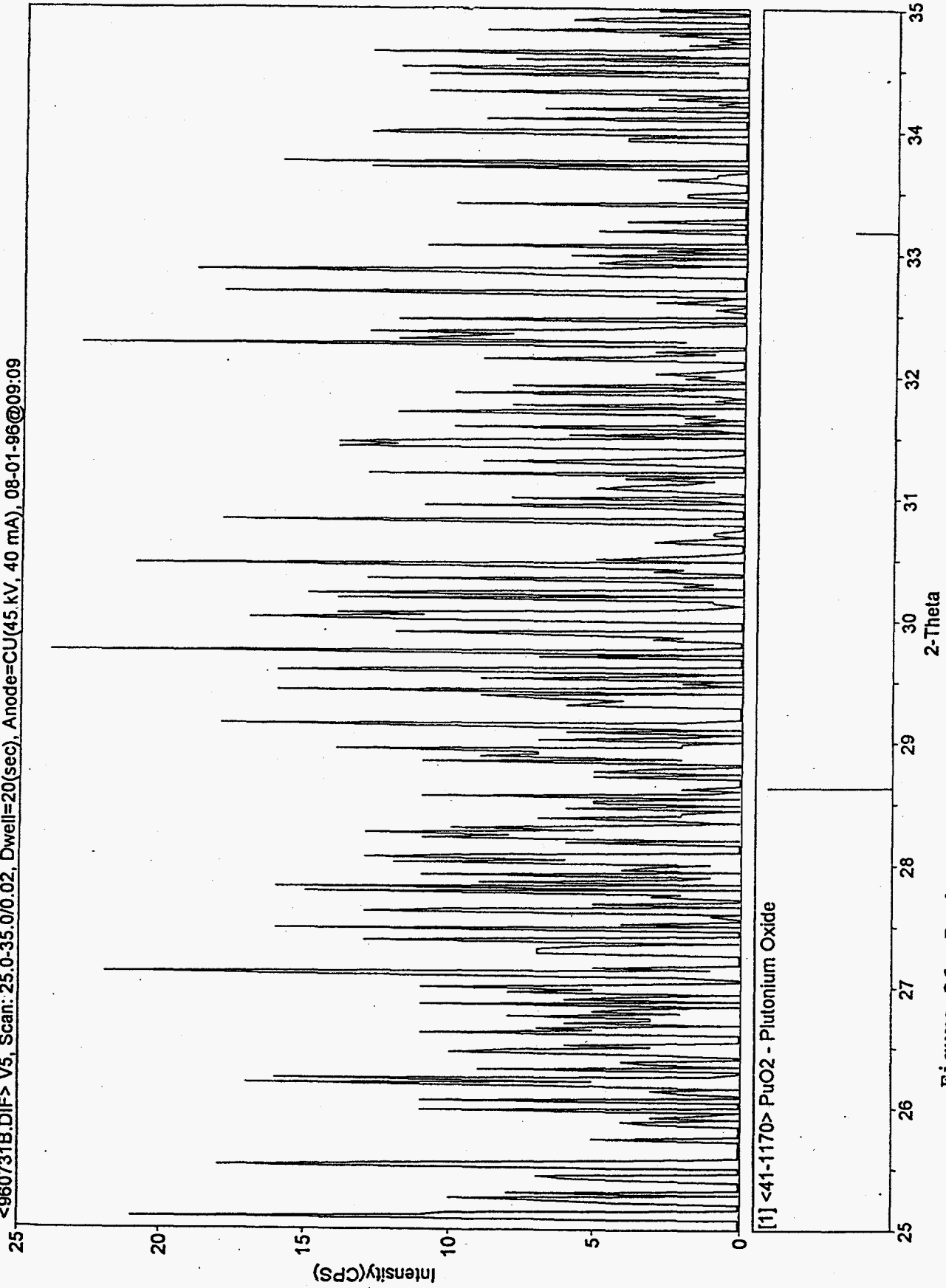


Figure 26. Background subtracted XRD plot for sample V5, 25 to 35 degrees 2-theta. "Stick Figure" display of PuO<sub>2</sub> pattern shown.

<960730B.DIF> V6, Scan: 25.0-35.0/0.02, Dwell=20(sec), Anode=CU(45 kV, 40 mA), 07-31-96@08:17

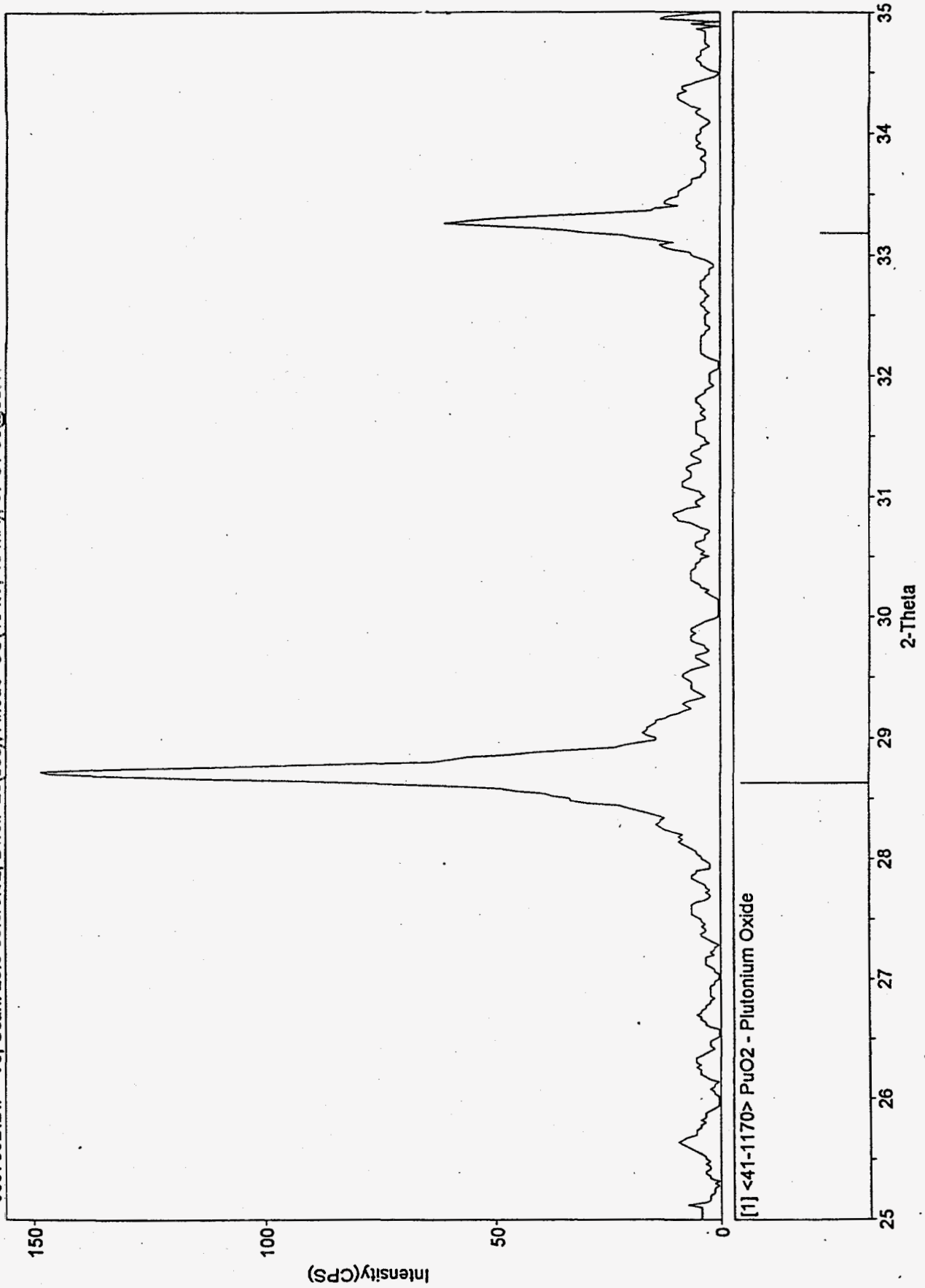


Figure 27. Background subtracted XRD plot for sample V6, 25 to 35 degrees 2-theta. "Stick Figure" display of PuO<sub>2</sub> pattern shown.

<960801B.DIF> V7, Scan: 25.0-35.0/0.02, Dwell=20(sec), Anode=CU(45 kV, 40 mA), 08-02-96@08:03

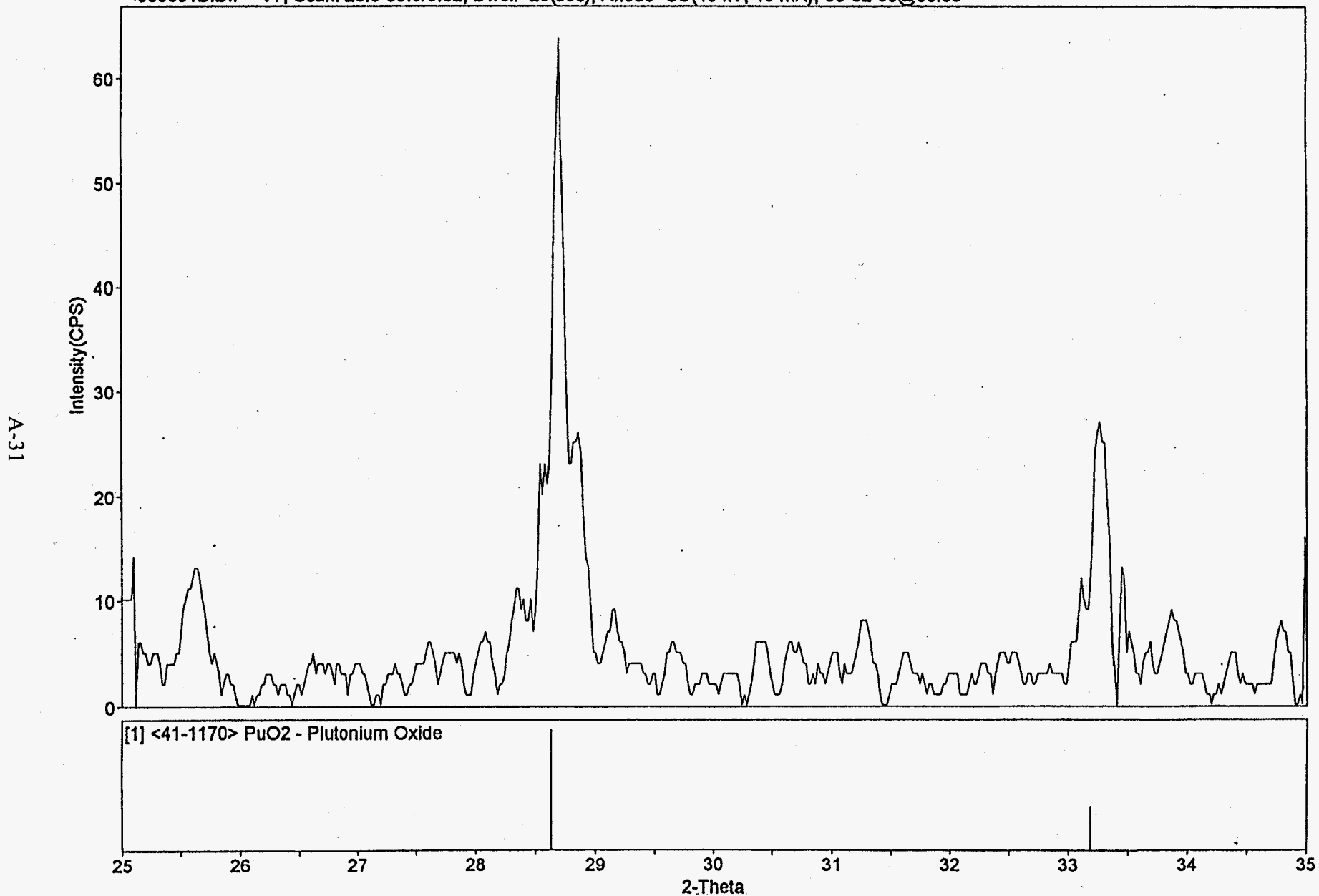


Figure 28. Background subtracted XRD plot for sample V7, 25 to 35 degrees 2-theta. "Stick Figure" display of PuO<sub>2</sub> pattern shown.

<960805A.RD> 3% PuO2, GLASS, Scan: 27.0-34.0/0.02, Dwell=20(sec), Anode=CU(45 kV, 40 mA), 08-05-96@09:46

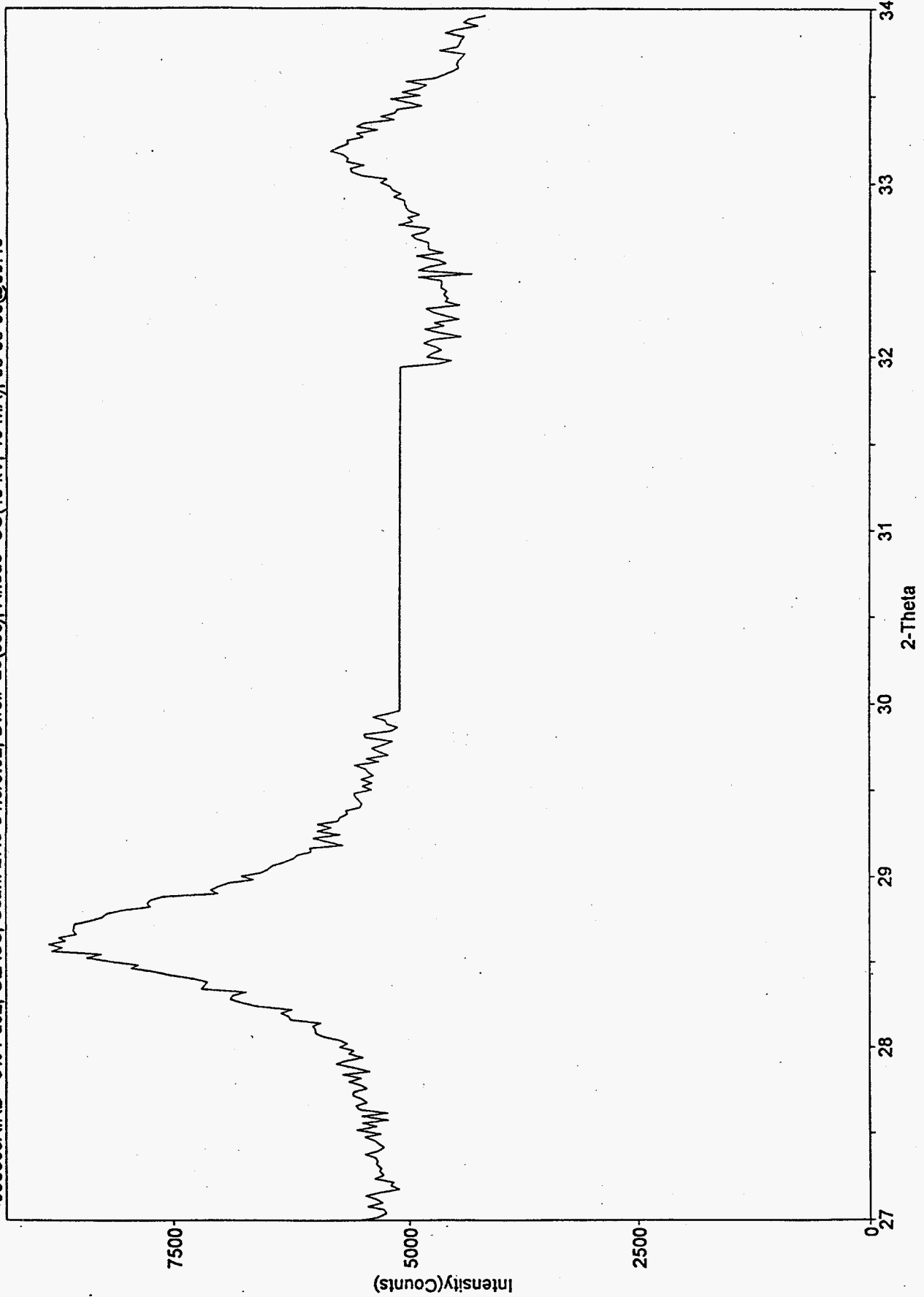


Figure 29. Raw data plot from sample of 3% PuO<sub>2</sub> in glass.

<960911A.RD> V8, 4 hr, 1550 deg, stirred, high fired, Scan: 5.0-75.0/0.05, Dwell=3(sec), Anode=CU(45 kV, 40 mA), 09-11-96@10:55

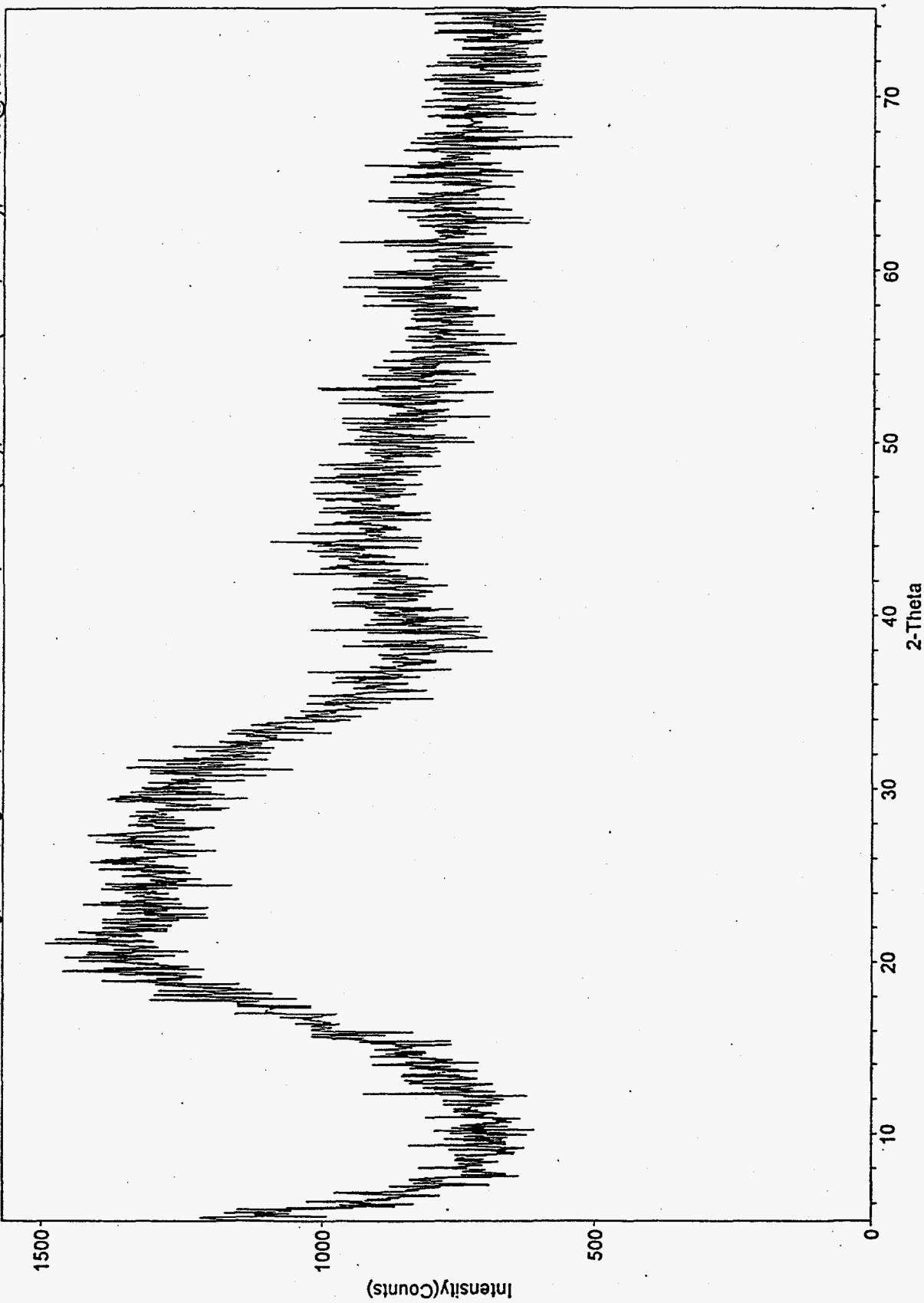


Figure 30. Raw XRD plot for sample V8, 5 to 75 degrees 2-theta.

<960911B.RD> V8, 4 hr, 1550 deg, stirred, high fired, Scan: 25.0-35.0/0.02, Dwell=20(sec), Anode=CU(45 kV, 40 mA), 09-12-96@08:22

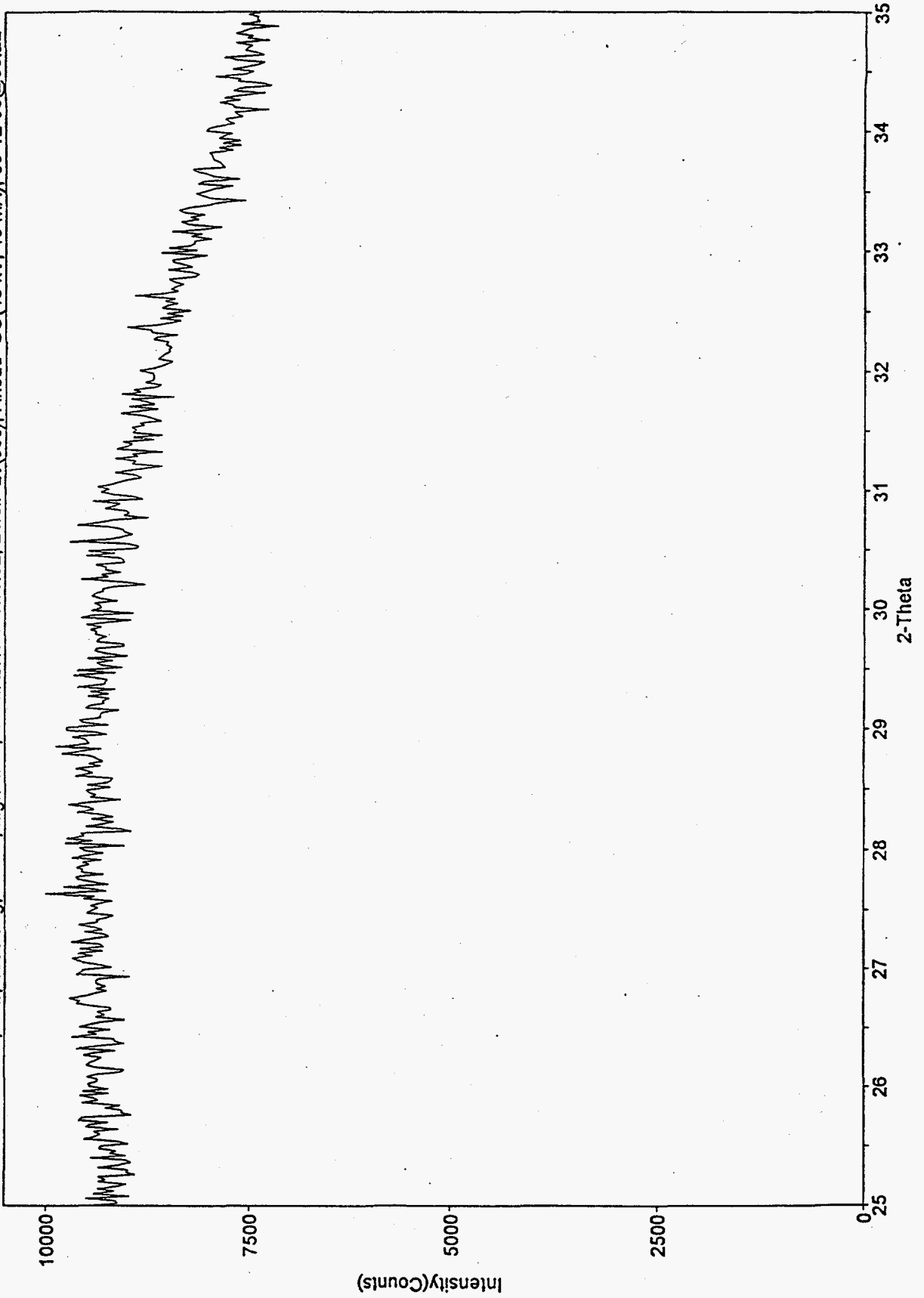


Figure 31. Raw XRD plot for sample V8, 25 to 35 degrees 2-theta.



<960911A.DIF> V8, 4 hr, 1550 deg, stirred, high fired, Scan: 5.0-75.0/0.05, Dwell=3(sec), Anode=Cu(45 kV, 40 mA), 09-11-96@11:03

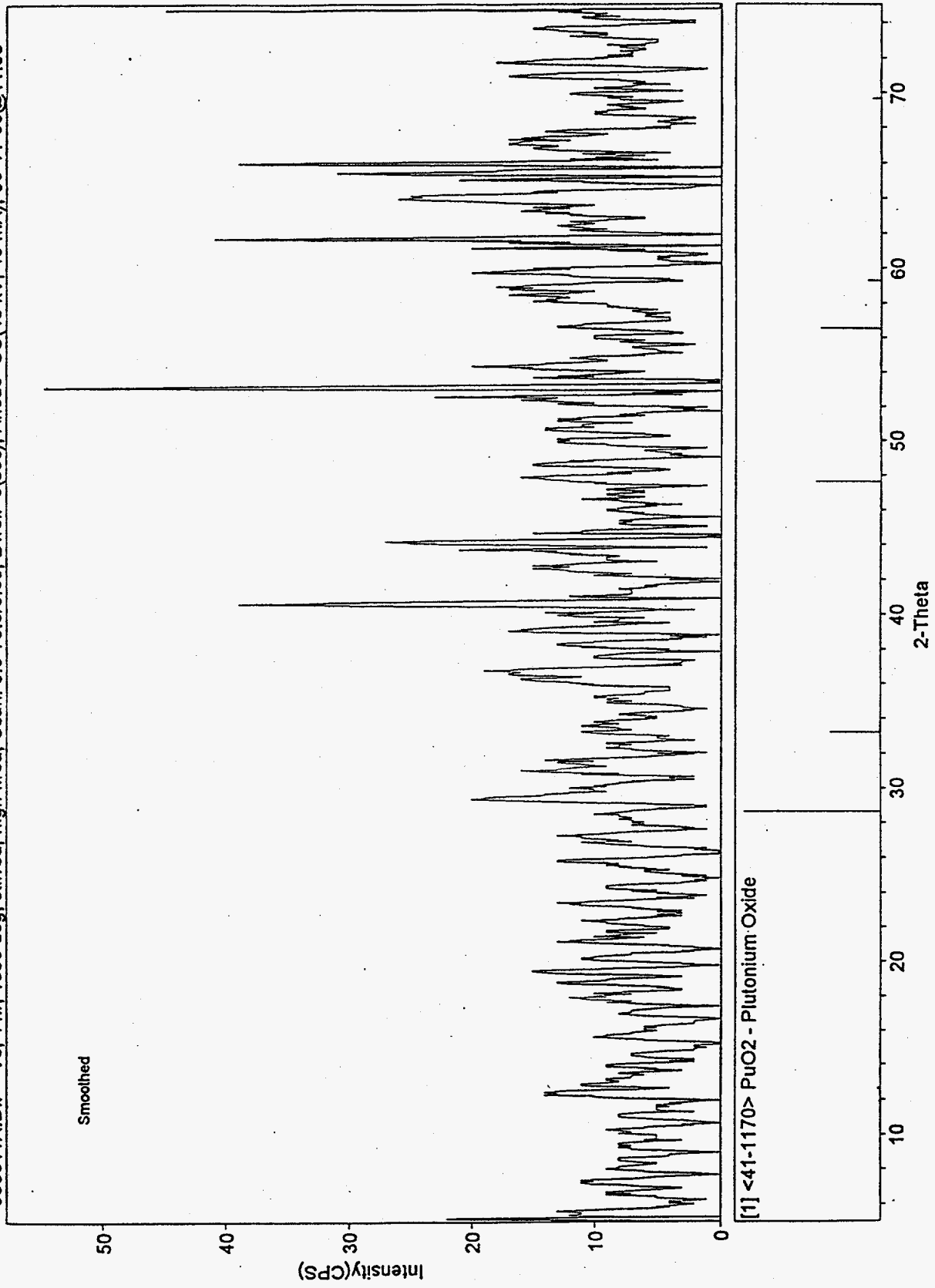


Figure 32. Background subtracted XRD plot for sample V8, 5 to 75 degrees 2-theta. "Stick Figure" display of PuO<sub>2</sub> pattern shown.

<960911B.DIF> V8, 4 hr, 1550 deg, stirred, high fired, Scan: 25.0-35.0/0.02, Dwell=20(sec), Anode=CU(45 kV, 40 mA), 09-12-96@09:11

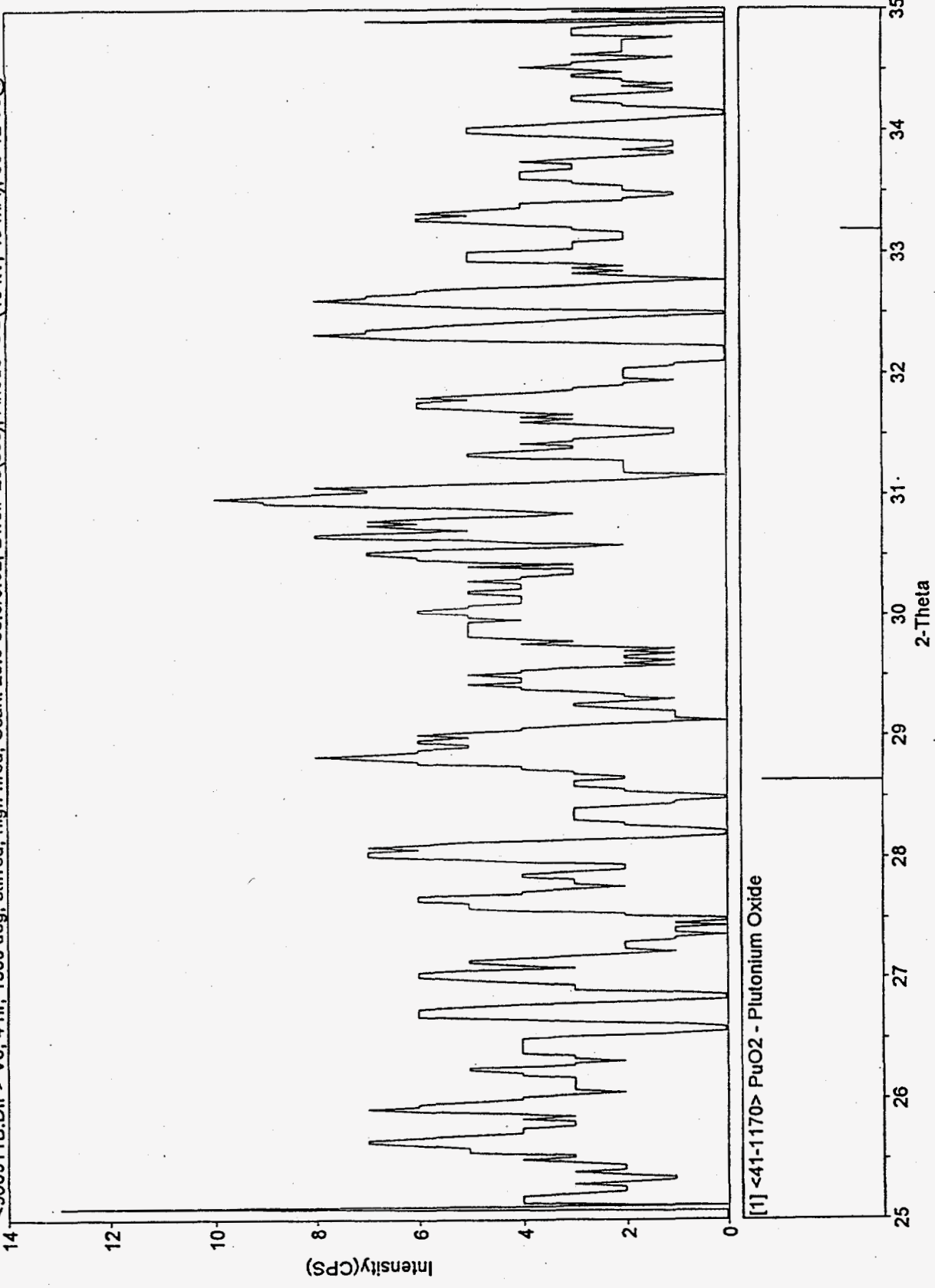


Figure 33. Background subtracted XRD plot for sample V8, 25 to 35 degrees 2-theta. "Stick Figure" display of PuO<sub>2</sub> pattern shown.

<960911A.RD> V8, 4 hr, 1550 deg, stirred, high fired, Scan: 5.0-75.0/0.05, Dwell=3(sec), Anode=CU(45 kV, 40 mA), 09-11-96@10:55

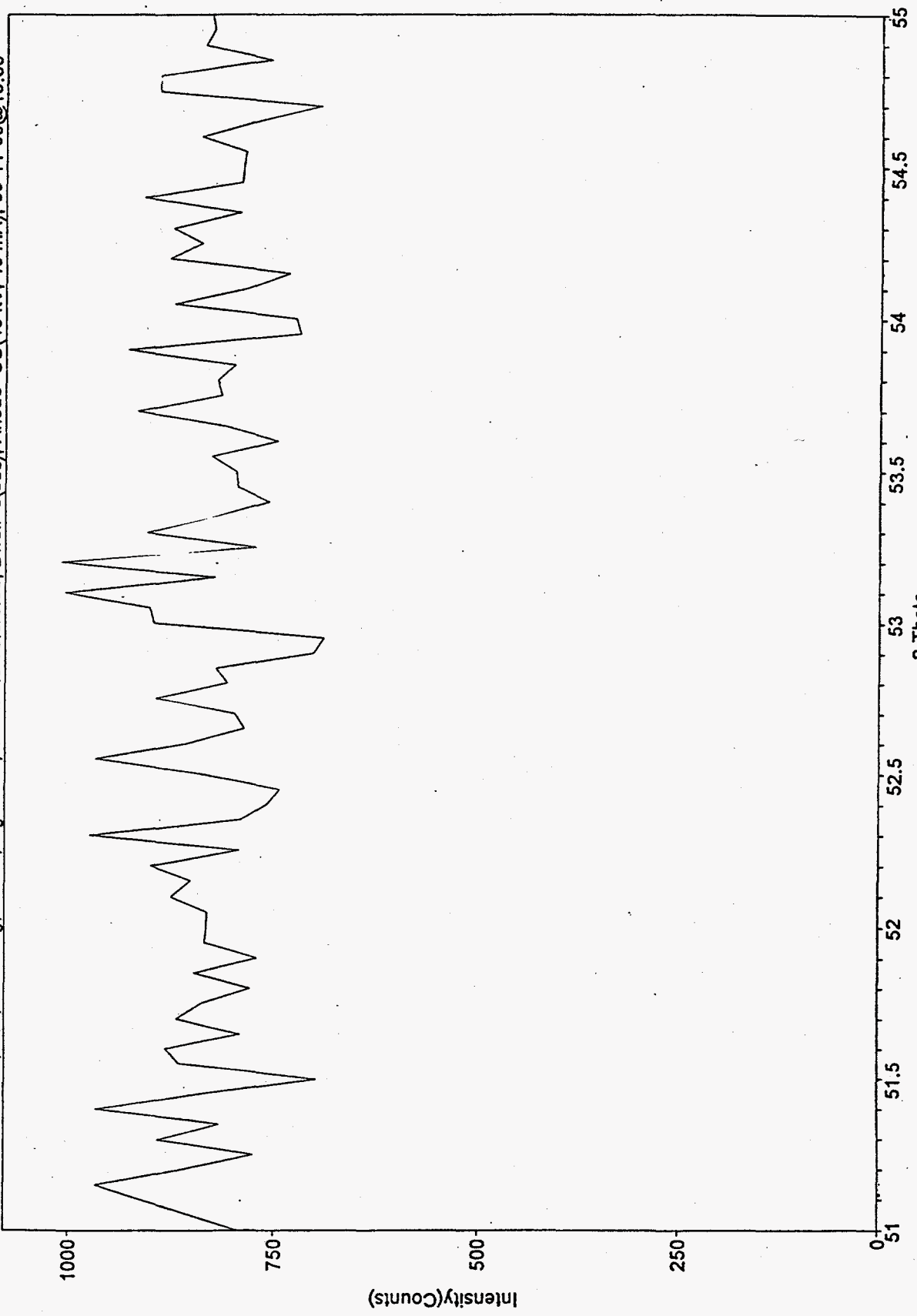


Figure 34. Raw xrd data plot for sample V8, detailed view of 53 degree range.

## **Appendix B**

### **Inductively Coupled Plasma/Mass Spectroscopy Results**

The following table shows the ICP/MS results from KOH fused glass samples listed in Table III. The glasses were prepared and analyzed according to the procedures listed in experimental approach section.

*James Brown*  
8/6/96

DATA REVIEW

Reviewed by: *[Signature]*

Date: 8/14/96 Pages: 1 of 1

John Vienna Analysis

August 2, 1996 (revised 8/6/96)

Results are reported in  $\mu\text{g/g}$  (ppm) of glass

The uncertainty of the results is conservatively estimated at  $\pm 15\%$ ; Al results are suspect due to unsatisfactory spike recovery

Sample Number	ICP/MS Number	Sample Weight (g)	B $\mu\text{g/g}$	Al $\mu\text{g/g}$	Sr $\mu\text{g/g}$	Zr $\mu\text{g/g}$	La $\mu\text{g/g}$	Nd $\mu\text{g/g}$	Gd $\mu\text{g/g}$	Pu-239 $\mu\text{g/g}$	Am-241 $\mu\text{g/g}$
1%HNO3	6802a1		0.56	<1	0.09	0.52	0.061	0.15	0.13	<0.0001	<0.0001
Process Blank	6802a14		360	<1000	240	14	9	390	180	<10	<10
Vienna-1	6802a15	0.1496	28000	(118000)	17600	6880	82600	90900	58100	76200	271
Vienna-1 Dup.	6802a23	0.1496	30100	(120000)	19300	7020	92800	106000	69500	78900	280 $\pm$ 30
Vienna-1 + Spike	6802a24	0.1496	106000	(217000)	89900	78700	168000	178000	136000	106000	646
Spike Recovery			114%	145%	106%	107%	112%	108%	99%	101%	94%
Vienna-2	6802a16	0.1026	32400	(117000)	19500	7830	97200	100000	67600	81100	329
Vienna-3	6802a17	0.1421	29100	(107000)	15800	6490	78800	87300	55100	76000	362
Vienna-4	6802a18	0.1498	31000	(119000)	18200	7080	85400	96800	59100	66500	249
Vienna-5	6802a19	0.1204	32600	(115000)	18300	6480	88000	94700	63400	71800	262
<b>CCV results are in ng/ml (ppb)</b>											
10ppb ICPMS-1	6802a7						9.41	10.3	10.9		
10ppb ICPMS-1	6802a20						10.0	8.19	9.74		
50 ppb Sr, Al I.V.	6802a8			47.3	52.5						
50 ppb Sr, Al I.V.	6802a21			45.6	58.5						
2ppb Pu-239	6705a4									1.94	
2ppb Pu-239	6705a16									2.02	
2ppb Pu-239	6805a26									2.21	
0.03ppb Am-241	6705a4										0.029 $\pm$ 0.005
0.03ppb Am-241	6705a16										0.039 $\pm$ 0.019
0.3ppb Am-241	6805a25										0.266

A-39

## Appendix C

### Radiochemical Analysis Results

The following tables show the alpha and gamma energy results from the starting Pu Nitrate feed solution and alpha energy and mass spectroscopy results from KOH fused glass samples listed in Table III. The glasses were prepared and analyzed according to the procedures listed in the experimental approach section.

Battelle Pacific Northwest National Laboratory  
 Analytical Chemistry Laboratory  
 Radiochemistry Group - 325 Bldg.

96-4817  
 7/3/96

Client: MJ Schweiger/D Haggard  
 WP #: K45603

Cognizant Scientist: L R Greenwood

Date: 7-3-96

Review: D. K. Adoff

Date: 7/3/96

Measured Activities (uCi/ml)

A-41

ALO ID Client ID	Alpha Energy Analysis				Gamma		Energy Analysis		
	Pu-238 Error +/-	Pu-239/240 Error +/-	Am-241 Error +/-	Cm-243/244 Error +/-	Am-241 Error +/-	Pu-239 Error +/-	Pu-241 Error +/-	Th-228 Error +/-	Np-237 Error +/-
96-4924 Pu Solution 6/18/96	4.30E+01 10%	1.29E+03 4%	7.78E+01 3%	1.30E+01 6%	8.14E+01 2%	1.33E+03 2%	1.28E-01 3%	2.75E-03 9%	1.96E-03 18%
96-4924 Duplicate Pu Solution 6/18/96	5.05E+01 10%	1.32E+03 4%	7.97E+01 3%	1.37E+01 6%					
Standard		99%	105%						
Blank	<4.E-8	<4.E-8	4.94E-7 10%	1.60E-6 7%					

Notes: Pu-241 was detected via the short-lived daughter U-237. Np-237 identification is uncertain since only one gamma line was detected.

Pu Oxide

Calculation sheet for weight%		PuO2 mole		271 grams		Pu(NO3)4		487 grams	
t1/2	87.7	24480	6560	12.4	3.75E+05	4.33E+02	years		
sample	Pu238	Pu239	Pu240	Pu241	Pu242	Am241			
Pu#1	3.47E+07	1.68E+08	6.46E+07	1.92E+08	6.05E+05	1.31E+07	dpm		
Pu#2	3.53E+07	1.80E+08	6.78E+07	1.98E+08	6.08E+05	1.37E+07	dpm		
Pu#3	3.67E+07	1.51E+08	7.06E+07	1.92E+08	6.34E+05	1.46E+07	dpm		
weight%	0.066%	85.692%	9.335%	0.050%	4.857%	0.125%	100.00%		
weight fra/g	0.000576	0.755734	0.0826732	0.0004491	0.04337	0.002227	0.88503 sum mas		
iso mass avg	6.53E-05	8.53E-02	9.29E-03	5.02E-05	4.83E-03	1.25E-04	avg mas	0.0996	
iso mass #1	0.000064	0.086150	0.008867	0.000050	0.004750	0.000118	mass #1	0.099998 g	
iso mass #2	0.000065	0.092245	0.009303	0.000051	0.004773	0.000124	mass #2	0.106560 g	
iso mass #3	0.000067	0.077391	0.009696	0.000050	0.004974	0.000132	mass #3	0.092310 g	

*[Signature]*

Cognizant scientist

9-13-96

Date



Battelle Pacific Northwest National Laboratory  
Analytical Chemistry Laboratory  
Radiochemistry Group - 325 Bldg.

96-5179  
7/12/96

Client: J Vienna  
Wp #: K42929

Cognizant Scientist:

Richard T. Tz

Date: 7/12/96

Concur :

T Trang-l

Date: 7/12/96

Measured Activities (uCi/g)

<u>ALO ID</u>	<u>Total Alpha</u>
<u>Client ID</u>	<u>Error %</u>
96-5179Pb	8.66E-3
Vienna 1 process Blank	21%
96-5179	7.47E 3
Vienna 1	6%
96-5180	7.45E 3
Vienna 2	6%
96-5181	7.26E 3
Vienna 3	6%
96-5182	6.15E 3
Vienna 4	6%
96-5183	7.21E 3
Vienna 5	6%
96-5183Dup	7.34E 3
Vienna 5	6%
Standard	115%
Blank	<2. E-3

Battelle Pacific Northwest National Laboratory  
Analytical Chemistry Laboratory  
Radiochemistry Group - 325 Bldg.

96-5179  
8/13/96

Client: J. Vienna  
WP #: K45606

Cognizant Scientist:

L. R. Greenwood

Date :

8-13-96

Review :

D. K. Adoff

Date :

3/13/96


Thermal Ionization Mass Spectrometry  
Mass %

ALO ID Client ID	Pu-238	Pu-239	Pu-240	Pu-241	Pu-242
96-5179 Vienna-1	0.012	93.340	6.411	0.194	0.043
96-5180 Vienna-2	0.011	93.349	6.415	0.189	0.036
96-5181 Vienna-3	0.015	93.362	6.387	0.197	0.039
96-5182 Vienna-4	0.013	93.383	6.375	0.193	0.036
96-5183 Vienna-5	0.014	93.338	6.415	0.190	0.042
Standard -Measured NBS SRM 946 Values	0.215 0.210	85.536 85.567	12.420 12.400	1.249 1.242	0.580 0.582

Pu glass 2nd run

Calculation sheet for weight%	PuO2 mol		271 grams			
t1/2	87.7	24480	6560	12.4	3.75E+05	4.33E+02 years
sample	Pu238	Pu239	Pu240	Pu241	Pu242	Am241
Pu#1	3.47E+06	1.15E+08	2.28E+07	1.75E+08	1.38E+05	3.44E+06 dpm

weight%	0.01433							
	0.010%	93.227%	4.961%	0.072%	1.730%	0.050%		100.00%
fra/g oxide	8.8E-05	0.822186	0.043933	0.000643	0.015448	0.000886		0.88318 Pu/Pu oxide
isotopic mass	0.00001	0.05920	0.00315	0.00005	0.00110	0.00003	sum mass	0.06353 g

 Cognizant scientist

9-13-96 Date

PuPNL30-11.4 3glass samples

Calculation sheet for weight%

PuO2 mol 271 grams

t1/2	87.7	24480	6560	12.4	3.75E+05	4.33E+02	years
sample	Pu238	Pu239	Pu240	Pu241	Pu242	Am241	
PuBG#2	3.62E+06	1.54E+08	1.90E+07	1.70E+08	1.04E+05	3.68E+06	dpm
Pu BC#1	5.60E+06	1.62E+08	1.36E+07	2.17E+08	1.27E+05	1.05E+07	dpm
Pu BC#2	4.40E+06	1.53E+08	1.91E+07	1.94E+08	1.01E+05	6.53E+06	dpm
weight%	0.010%	96.012%	2.859%	0.061%	1.059%	0.076%	100.00%
weight fra/g	8.76E-05	8.47E-01	2.53E-02	5.42E-04	9.46E-03	1.35E-03	Sum 0.88349
iso mass avg	5.92E-06	5.70E-02	1.70E-03	3.62E-05	6.28E-04	4.49E-05	avg mas 0.0594
PuBG#2 iso mass	4.71E-06	5.61E-02	1.87E-03	3.18E-05	5.90E-04	2.40E-05	mass #1 0.058558 g
Pu BC#1 iso mass	7.30E-06	5.91E-02	1.34E-03	4.05E-05	7.21E-04	6.84E-05	mass #2 0.061239 g
Pu BC#2 iso mass	5.73E-06	5.67E-02	1.88E-03	3.62E-05	6.74E-04	4.26E-05	mass #3 0.058194 g



Cognizant scientist

10-4-96

Date